NATIONAL TRANSPORTATION SAFETY BOARD
Office of Aviation Safety
Aviation Engineering Division
Washington, DC 20594

December 5, 2003

ADDENDUM NUMBER 3 TO THE STRUCTURES GROUP CHAIRMAN'S FACTUAL REPORT

DCA02MA001

A. ACCIDENT

Location:	Belle Harbor, NY
Date:	November 12, 2001
Time:	09:16:14 EST
Aircraft:	American Airlines Flight 587, Airbus Model A300-605R, N14053 Manufactures Serial Number (MSN) 420

B. STRUCTURES GROUP

Chairman: Brian K Murphy
National Transportation Safety Board
Washington, DC

C. AIRBUS REPORT

1. "AAL587 Airbus Structure Investigation, Accident Analysis – FEM RHS local rear lug model"

	Technical Note	

Report Nr.: TN – ESGC – 1018/03

Author:
Department.:

Title

AAL587 Airbus Structure Investigation

Accident Analysis - FEM RHS local rear lug model

Date: 08.12.2003

Summary:

At the RHS and LHS rear fin box attachments to the fuselage the 3D models were embedded in the global 2D model. This allows to investigate the influence of this very detailed idealization on the attachment loads for front, center and rear lug.
Additionally, it becomes possible to get a full 3D state of stress in the lug around the pin hole. The results (displacement) from the 2D analysis with both embedded 3D lugs were used as boundary conditions for the nonlinear contact analysis.

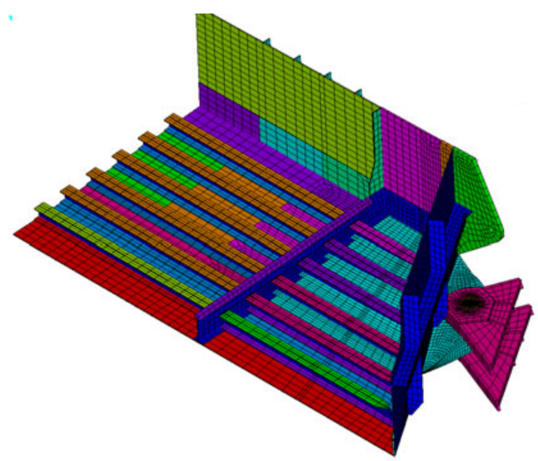

Public Docket	Issue	Date	No. of page	Revised pages	Valid from/for
	1	10.11.2003	42		
	2	02.12.2003	50	34-50 ; Format change DINA4 to LETTER	
	3	08.12.2003	50		

Table of contents

Table of contents, cont'd.

1. Introduction

At the RHS and LHS rear fin box attachments to the fuselage the 3D models were embedded in the global 2D model. This allows to investigate the influence of this very detailed idealization on the attachment loads for front, center and rear lug.
Additionally, it becomes possible to get a full 3D state of stress in the lug around the pin hole. The results (displacements) from the 2D analysis with both embedded 3D lugs were used as boundary conditions for the nonlinear contact analysis.

2. General VTP overview and the RHS rear main lug FEA model

Figure 2.1 shows the vertical stabilizer with the 3D RHS rear main lug FEA model.

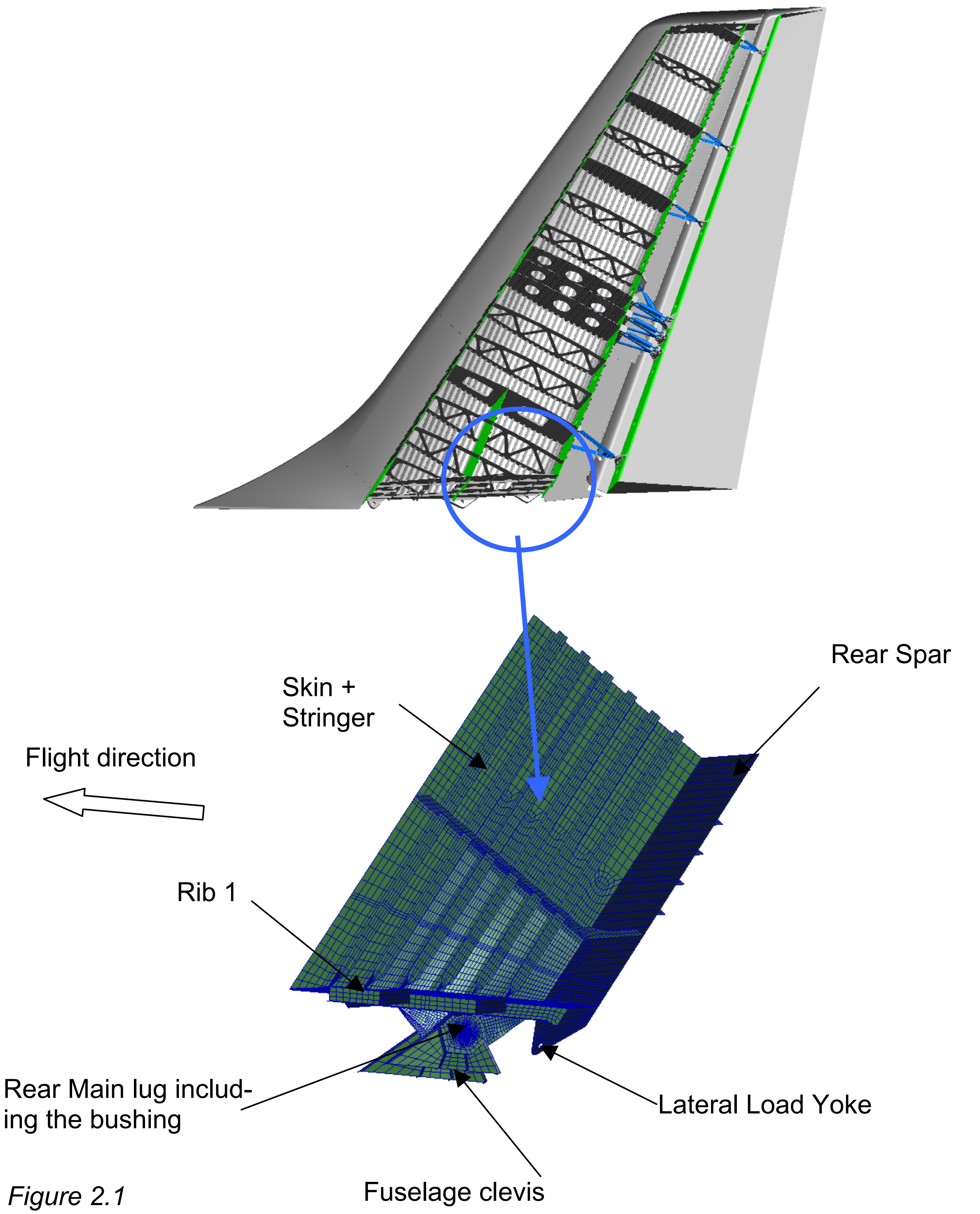

Figure 2.1

Figures 2.2 and 2.3 gives a detailed view of the smooth 3D lug area in the FEA-model.

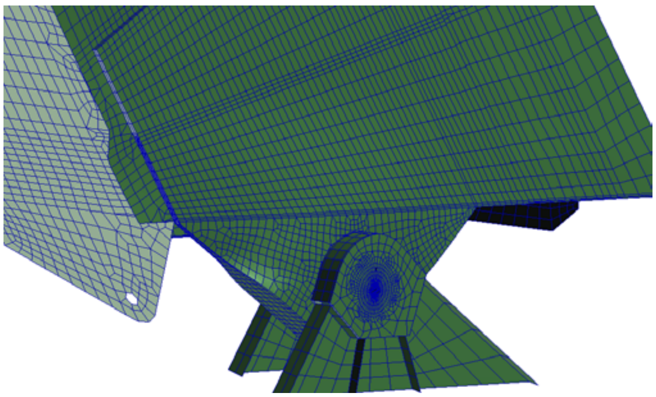

Figure 2.2

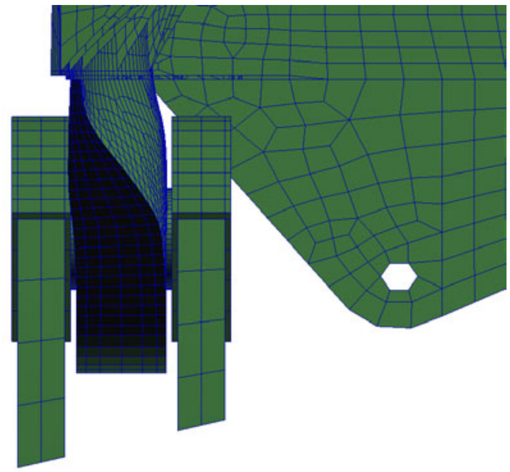

Figure 2.3

2.1.1 Skin panel

Figure 2.4 shows the skin panel section of the rear main lug from rear spar to stringer P5 and rib 1 to rib 4 which was modelled in the 3D rear main lug model. Figure 2.5 is a cross section through the skin panel and shows the principle build up of skin and stringer.

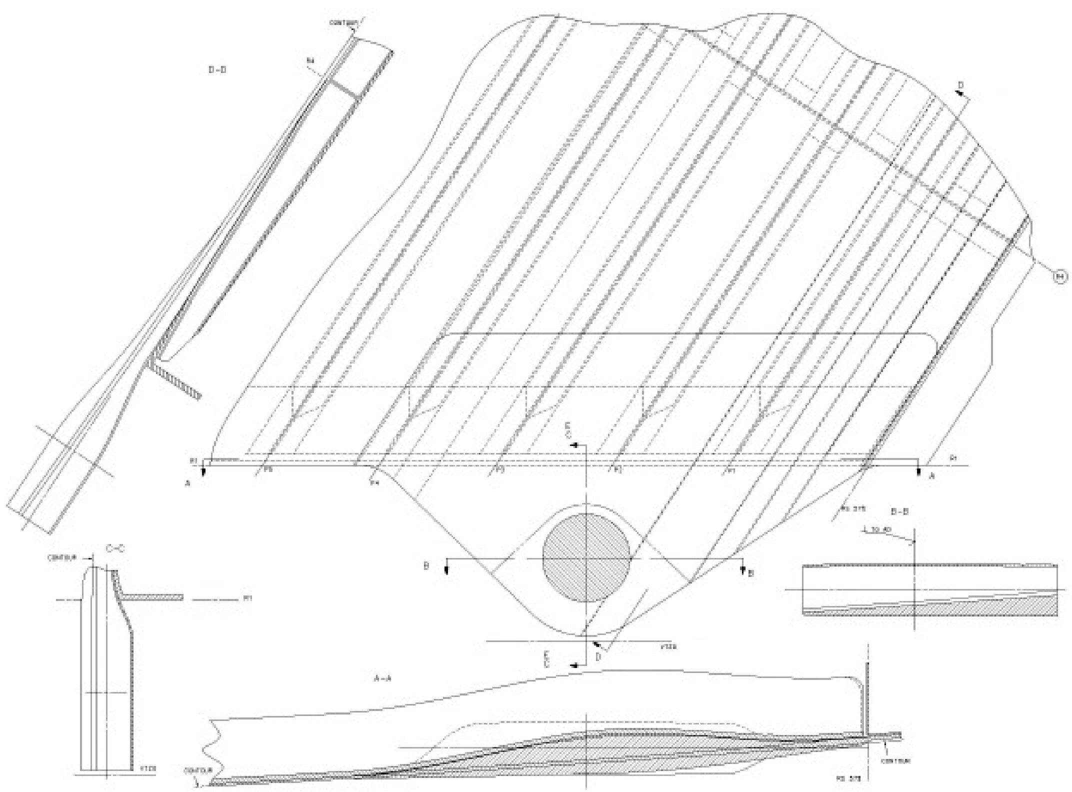

Figure 2.4

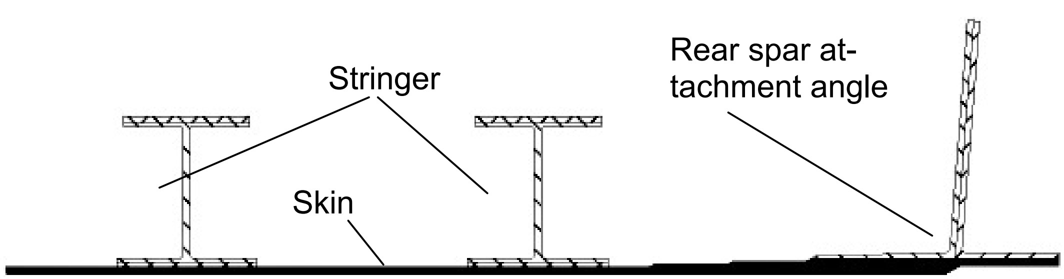

Figure 2.5

2.1.2 Rib 1 rear plate

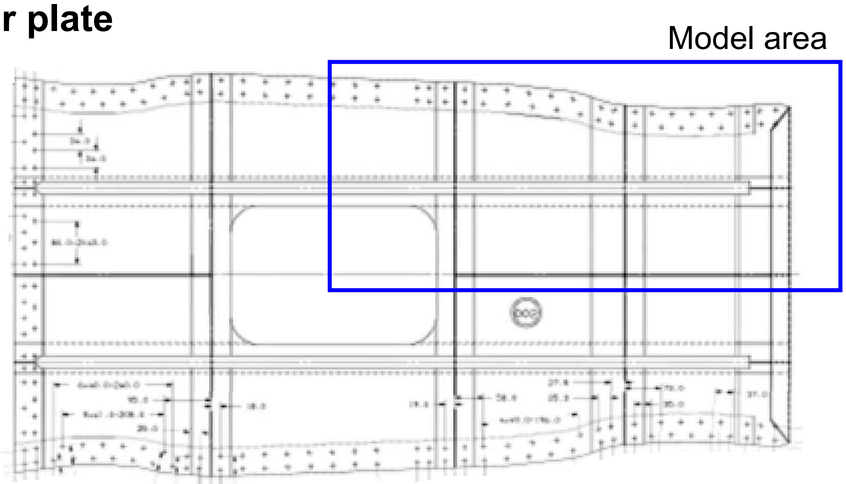

Figure 2.6

2.1.3 Rear spar section

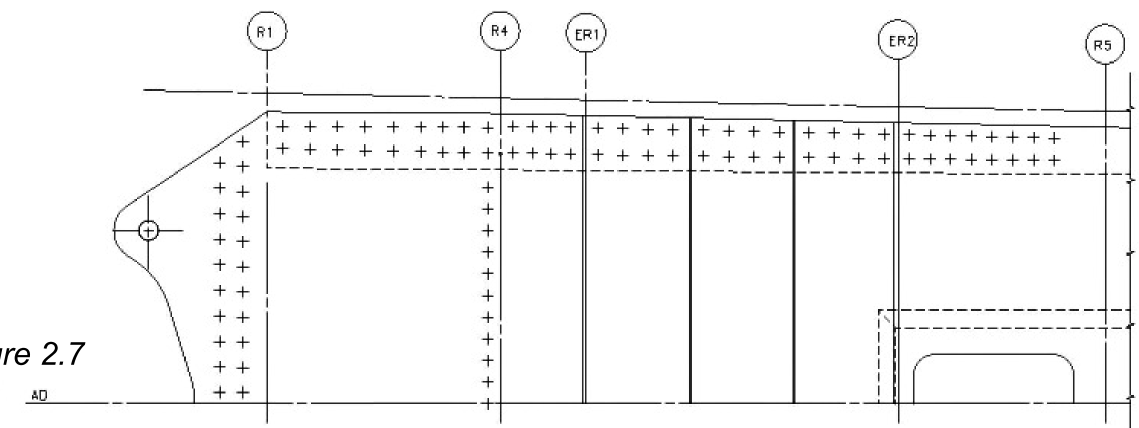

Figure 2.7

2.2 Fuselage/ fin connection bolt

The following figures 2.8 to 2.10 illustrate the fuselage / fin connection bolt components and assembly.

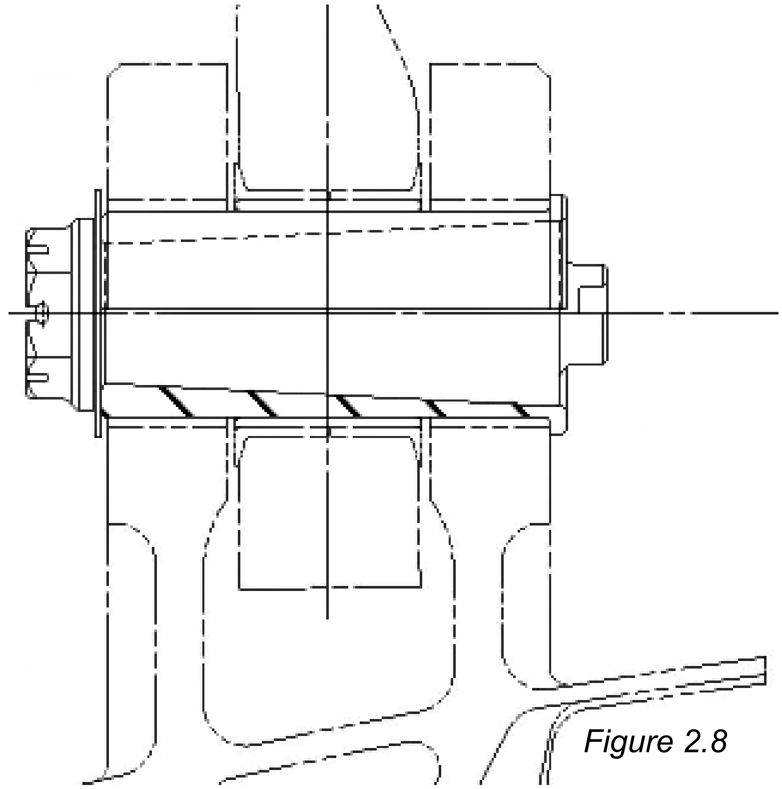

Figure 2.8

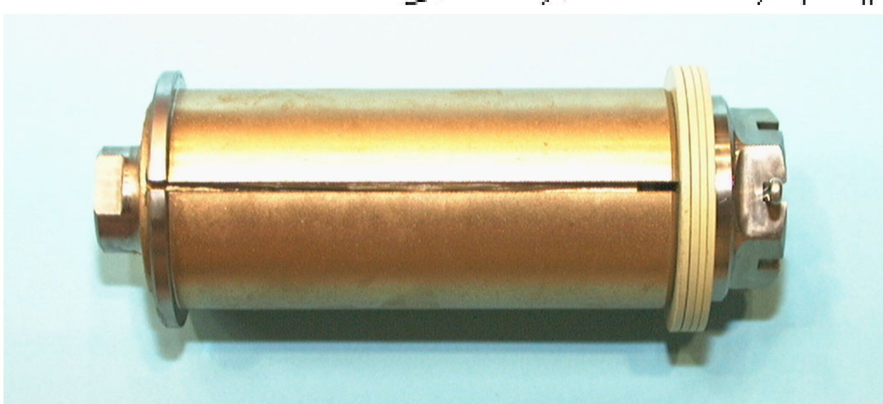

Figure 2.9

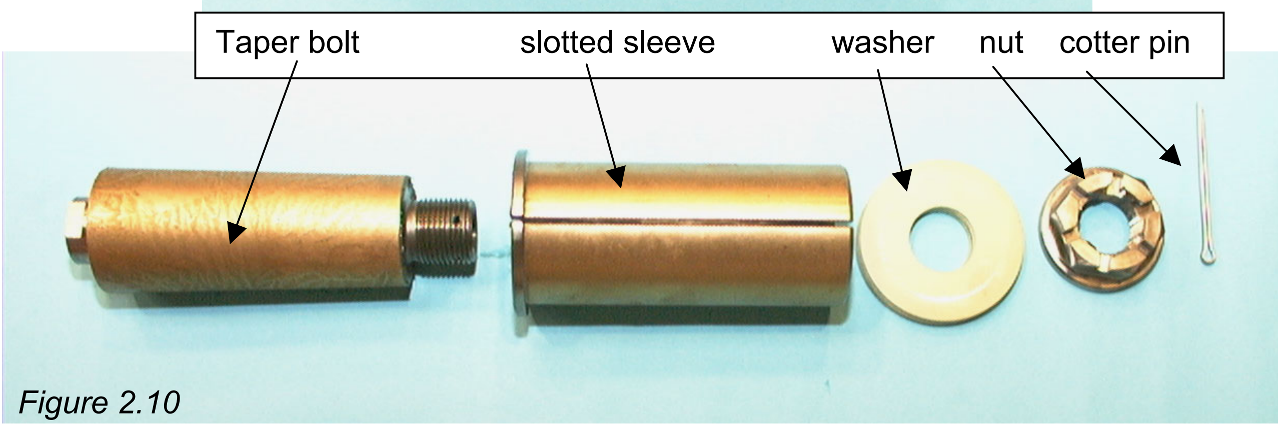

Figure 2.10

3. 2D RHS rear main fitting area FE-Idealization in the global analysis model

Detailed information about the 2D global NASTRAN (see figure 3.1) model is given in the report " *AAL587 Airbus Structure Investigation - Accident Analysis – FEM Global model VTP & Rudder*" TN – ESGC – 1017/03.

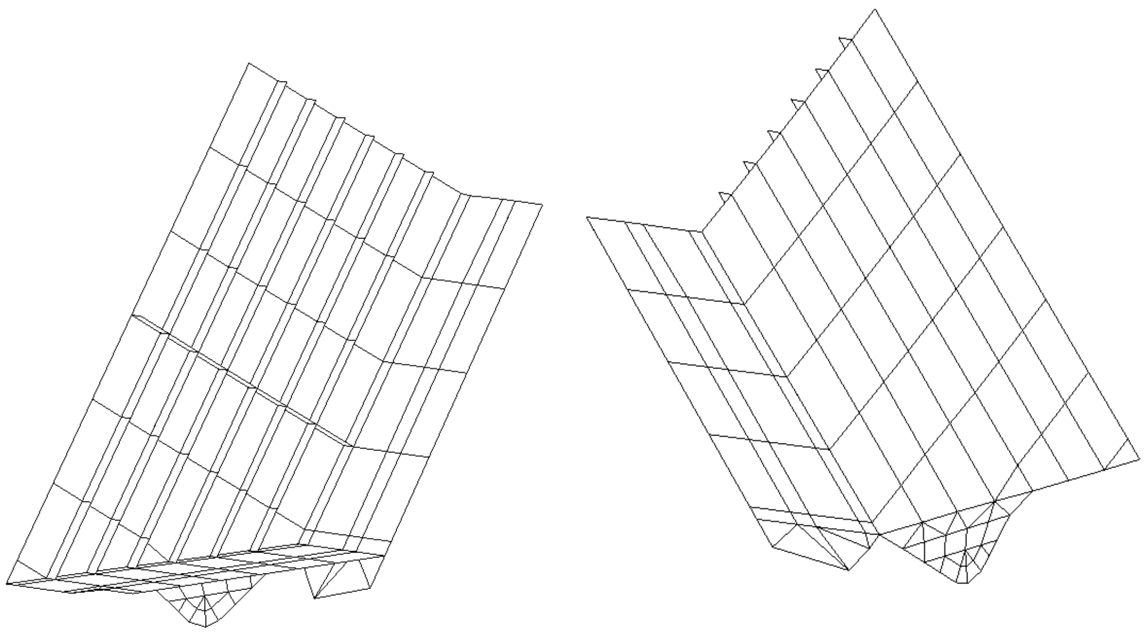

Figure 3.1

3.1 3D rear lug FEA model

The complete model (see figures 3.2 to 3.4) was developed in ANSYS and converted from the ANSYS FE-code into the NASTRAN FE-code. In order to take into account contact surface capabilities of ANSYS, all the nonlinear contact analyses are done with ANSYS.

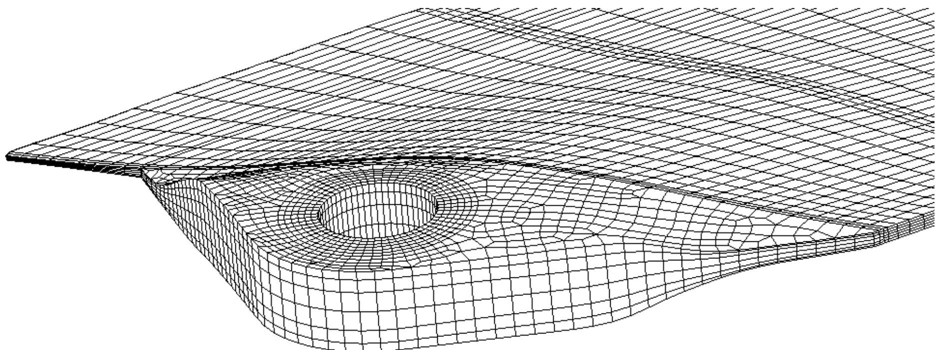

Figure 3.2

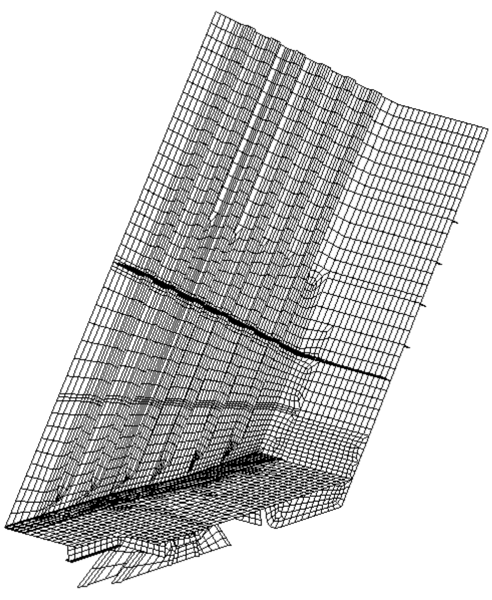

Figure 3.3

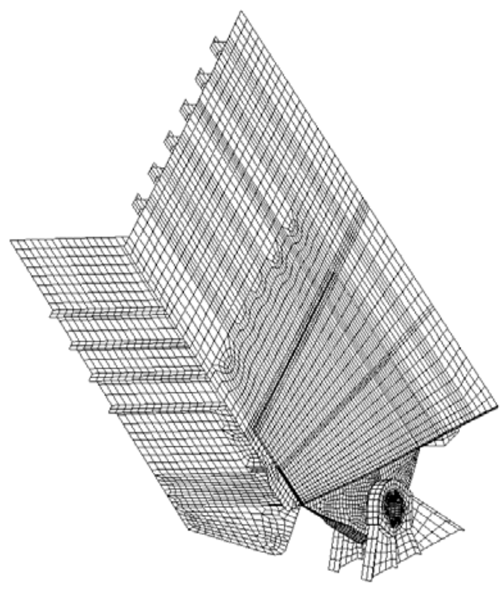

Figure 3.4

Components of the FE-model

The 3D RHS rear main lug model (see figure 3.5) consists of the following components:

- 3D CFRP solid lug
- Skin panel with Stringer (rib 1 to rib4 and rear spar to stringer P6)
- Rear Spar (portion of the rear spar and cut out at the VTP mid plane)
- Rib 1 (portion of the rib1 and cut out at the VTP mid plane)

and the fuselage clevis part which protrudes the fuselage surface.

The inner and outer fitting part including the skin area was modeled with solid elements. The remaining structure of the model is idealized with shell elements.

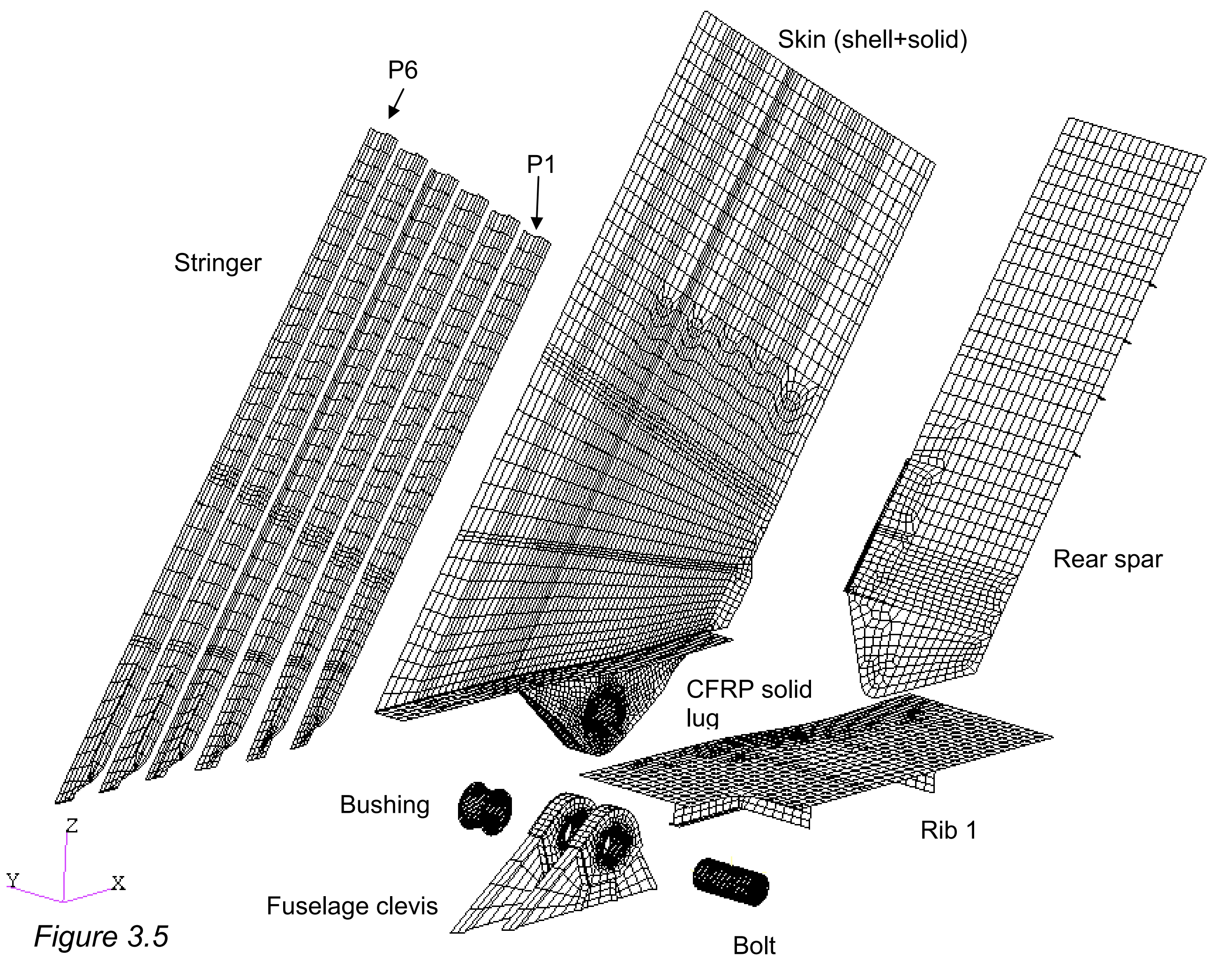

Figure 3.5

3.2 Global NASTRAN 2D VTP model with embedded LHS & RHS rear main fitting models

The 3D solid lug model (see figure 3.6 to 3.11) was embedded into the 2D global NASTRAN model. To embed the RHS & LHS rear main attachment fitting the RHS model was mirrored.

RHS 3D rear main fitting model

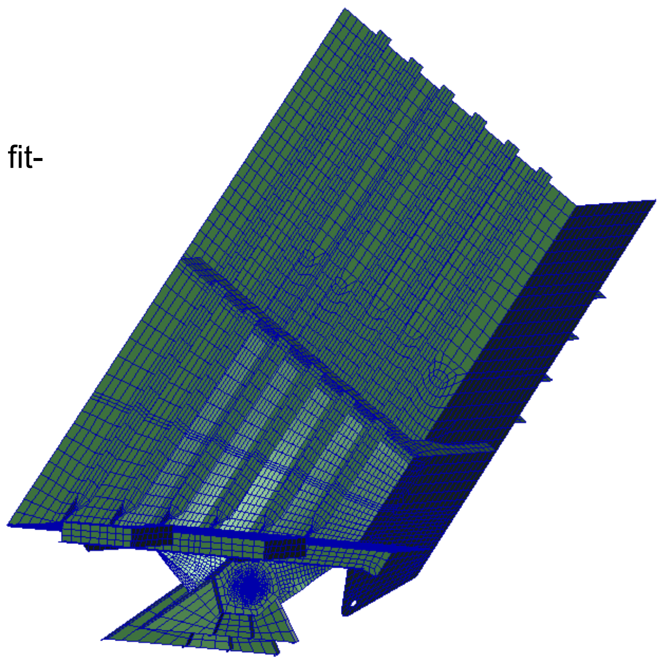

Figure 3.6

Figure 3.7

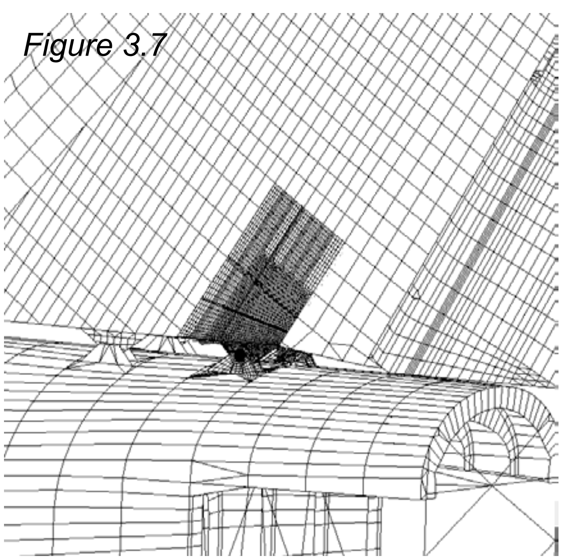

View on the embedded LHS 3D model

Figure 3.8

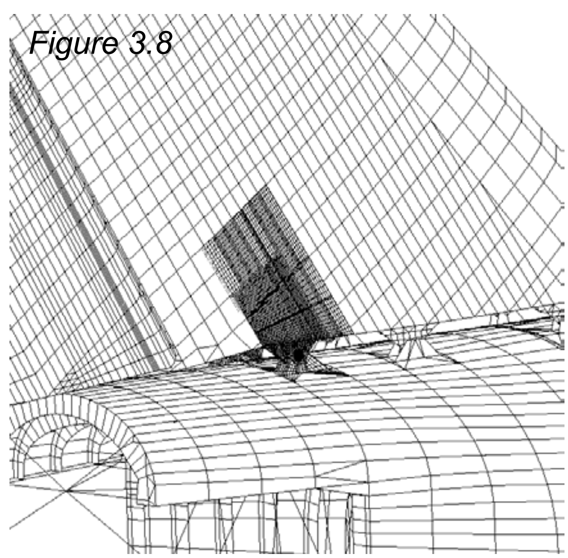

View on the embedded RHS 3D model

This page gives different views of the 3D rear main fitting model.

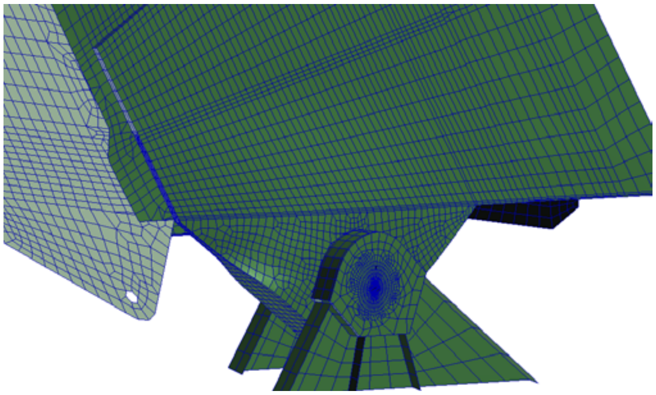

Figure 3.9

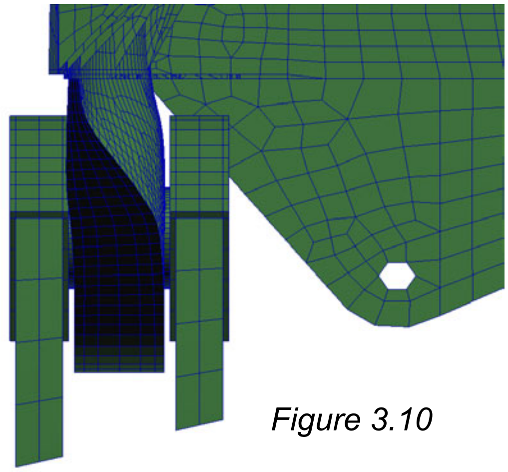

Figure 3.10

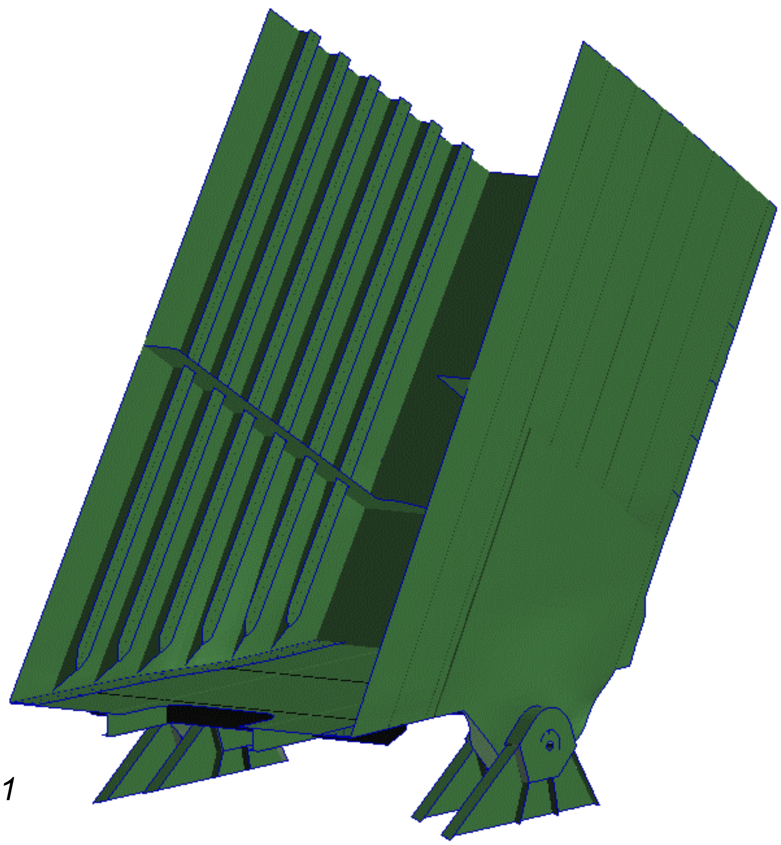

Figure 3.11

Complete 3D LHS & RHS rear main attachment fitting model

3.3 RBE2 interface elements between 2D and 3D model mesh

The fine mesh of the embedded 3D rear main fitting model is connected to the coarse mesh of the global 2D NASTRAN model (see figure 3.12 and 3.13). For the connection RBE2-Elements were used. The independent node of the coarse 2D mesh was connected to the nearest nodes of the 3D model mesh.

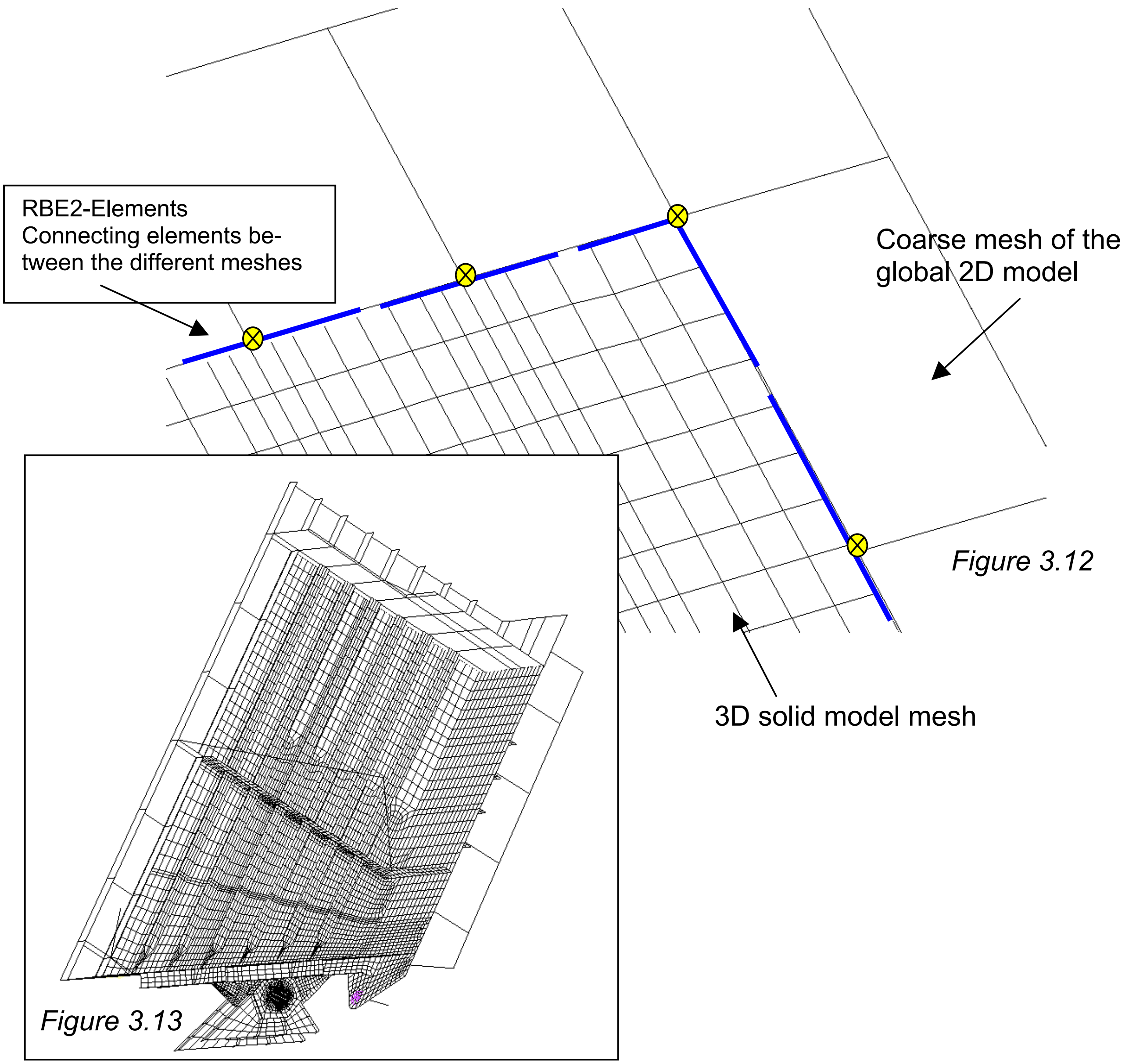

Figure 3.12

Figure 3.13

3.4 Fuselage clevis

The 3D ANSYS rear main fitting model includes a complete contact surface idealization in the fuselage / VTP connection bolt area.

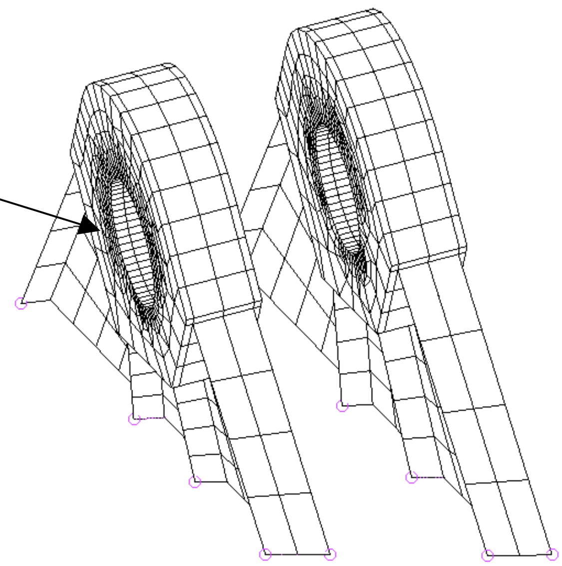

Figure 3.15

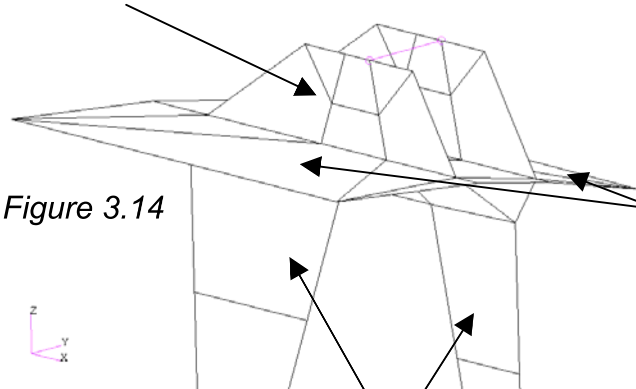

Figure 3.14

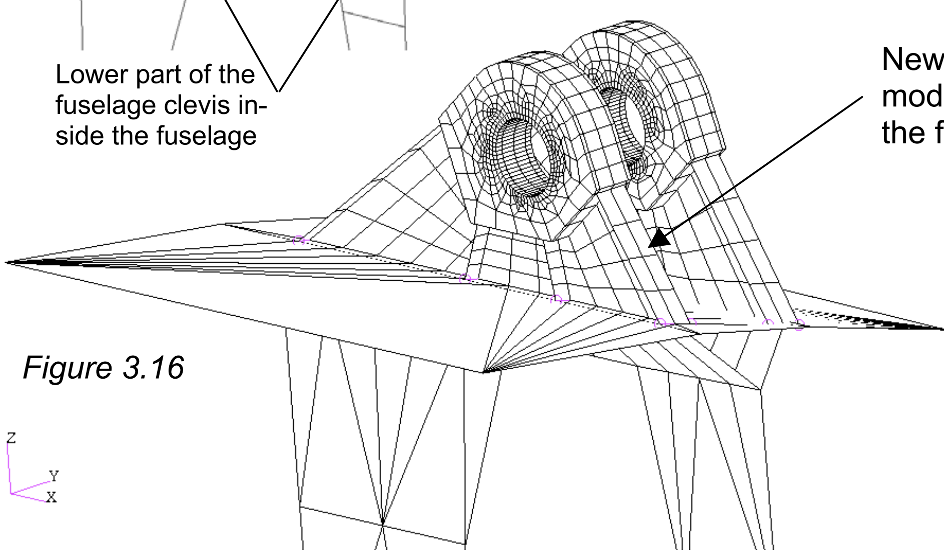

Figure 3.16

3.5 Lug reaction force & moment calculation in NASTRAN [linear static]

To calculate the main fitting reaction forces & moments the grid point force balance for the clevis to fuselage interface are used (see figure 3.17 and 3.18).

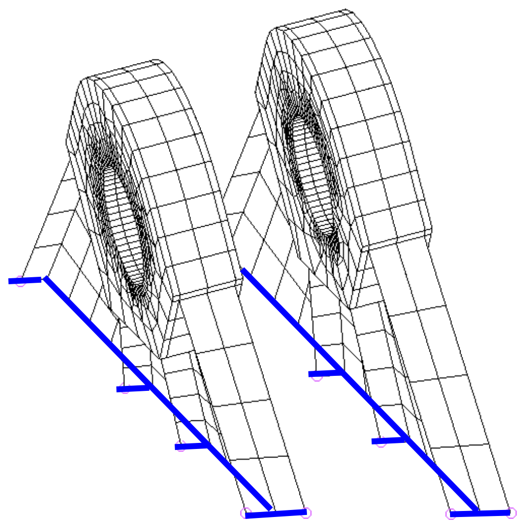

Figure 3.17

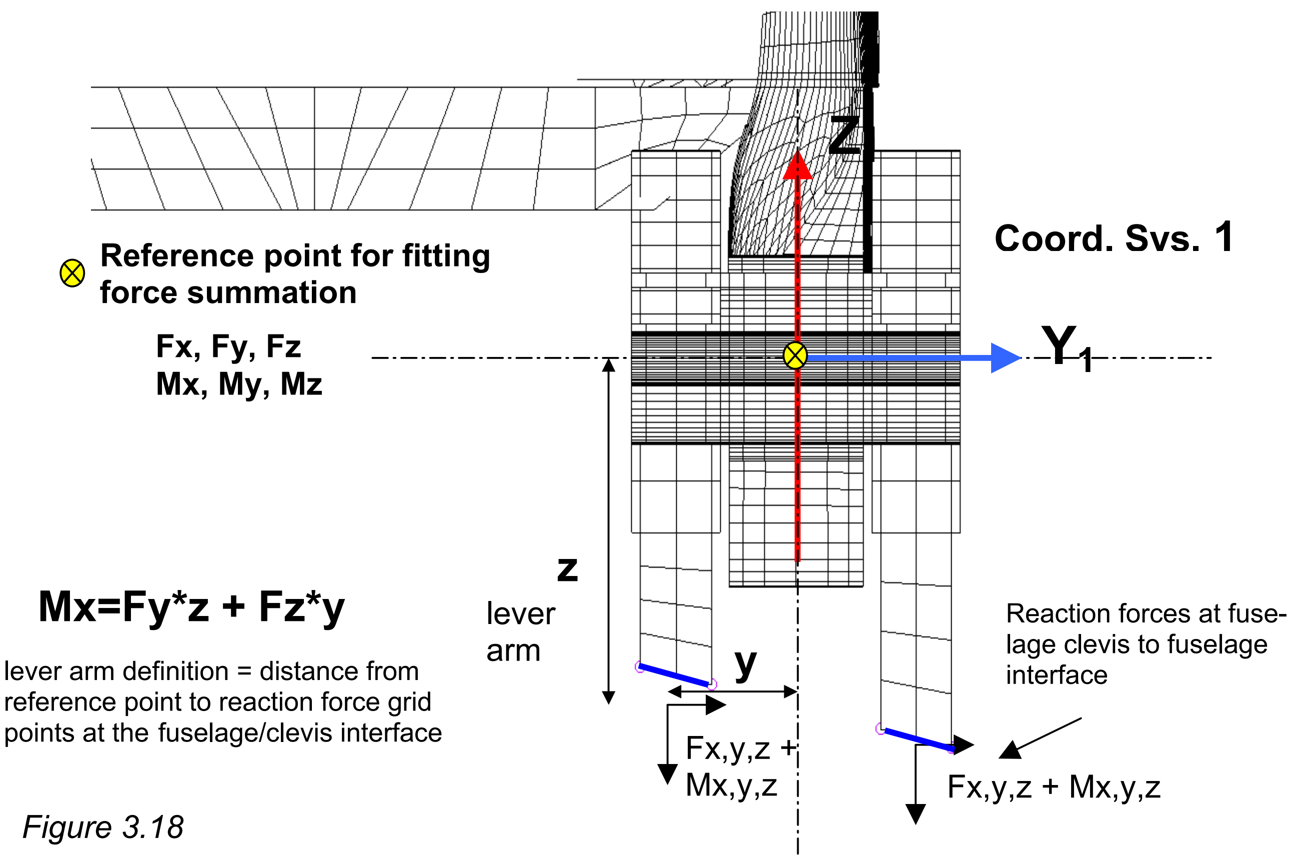

Figure 3.18

3.6 NASTRAN bolt bonding conditions *Cond I & II* [linear static]

In the first step of the NASTRAN analysis procedure the bolt for each, the LHS & RHS, 3D embedded model are completely (360°) bonded. With the so called bonding condition ***Cond I*** the angle of the resultant main fitting force relative to rib 1 (see figure 3.19) was calculated.

Table 3.1

	Cond I	**Cond II *)**
Fuselage clevis to bolt	360°	180°
Bolt to bushing	360°	180°
Bushing to CFRP lug	360°	180°

*) connection angle perpendicular to the resultant force direction

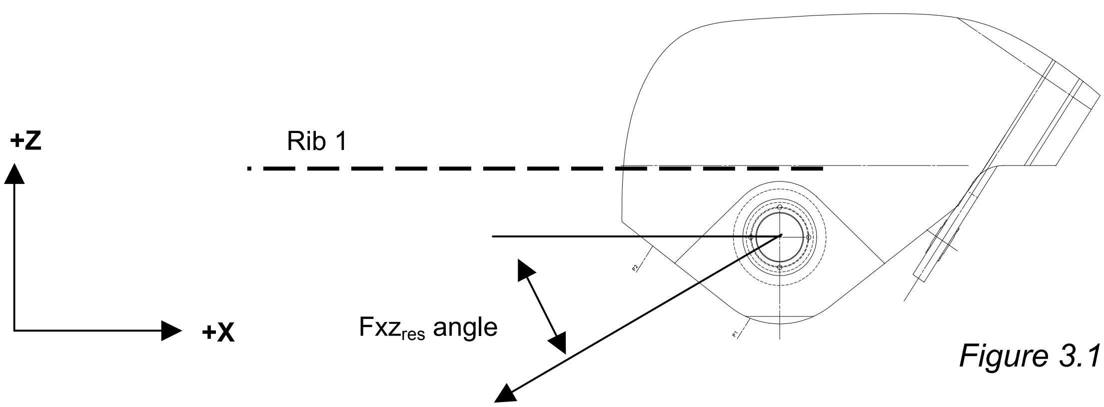

Figure 3.19

In the second NASTRAN analysis step the bolt is only bonded over 180°-degree corresponding to the Fres direction. Due to the tension and compression area of the connection different nodes have to be bonded. The figure 3.20 on the next page shows the necessary bonding procedure exemplary for a tension force at the rear main lug.

The 180°-degree bonding is the best approach to model the contact situation. Taking into account this bonding configuration, called ***Cond II***, the boundary displacement conditions for the ANSYS model and the local lug reactions are recalculated.

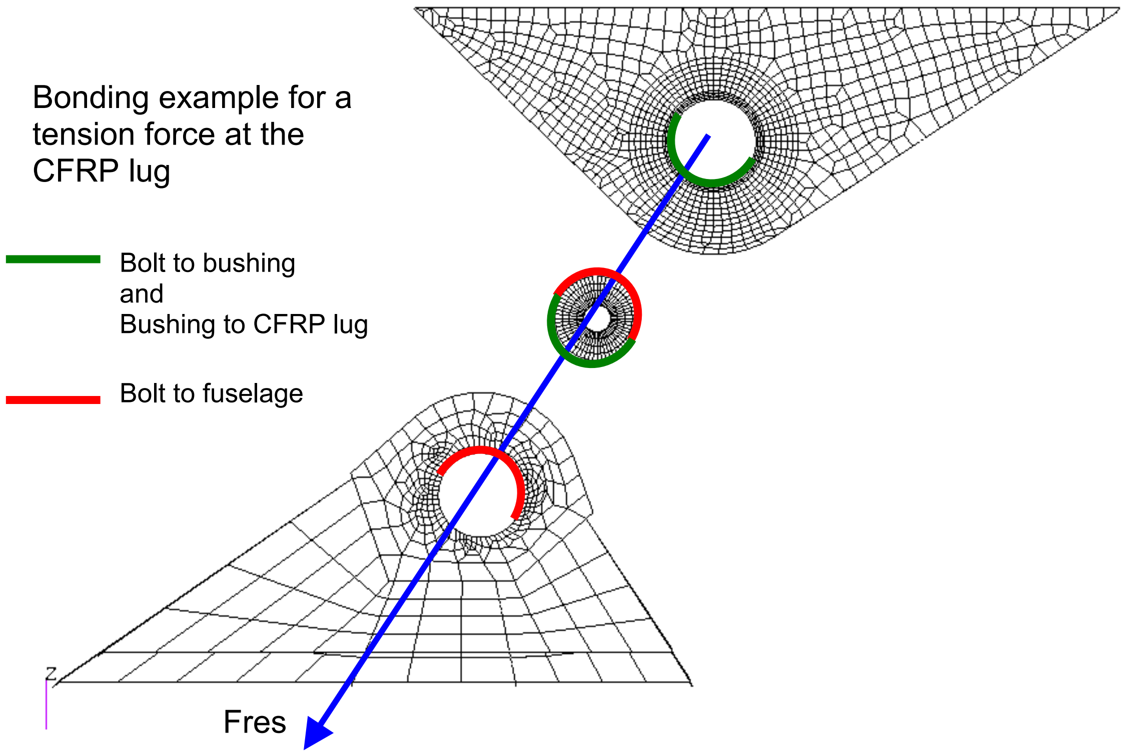

Figure 3.20

4. Results of the global model with embedded LHS & RHS 3D rear main fittings [NASTRAN / linear static]

4.1 Fin deformation under W375 accident loading condition

The max. fin deformation (see figure 4.1) with the embedded solid models (628mm at the rudder trailing edge) is nearly the same compared to the global 2D model (624mm).

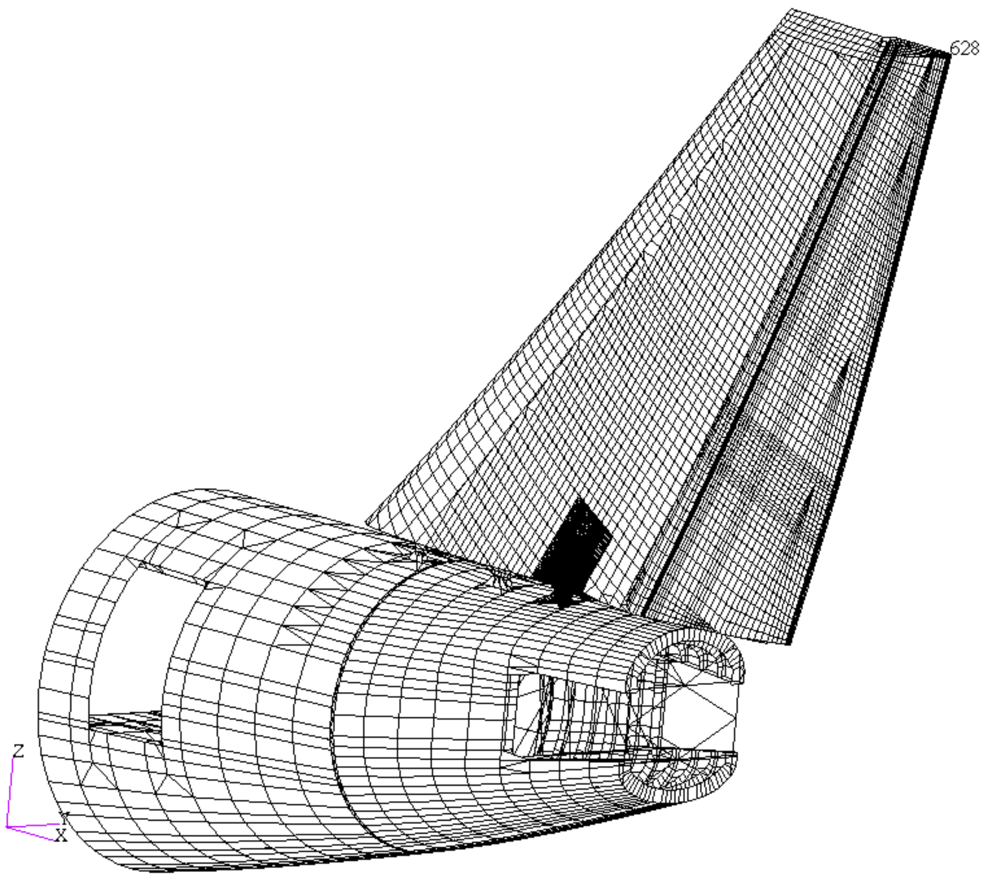

Figure 4.1

4.2 Fitting forces of W375 bonding *Cond I* [NASTRAN / linear static]

Rudder deflection angle	[°]	-11,47

Table 4.1 **Main Fitting Reaction Forces**

Embedded 3D rear main lug

	Front [N]		Centre [N]		Rear [N]	
	LHS	**RHS**	**LHS**	**RHS**	**LHS**	**RHS**
Fx	263250	-277060	253114	-262495	**420334**	**-396038**
Fy	8926	9319	30530	30991	**50474**	**43419**
Fz	316225	-333185	699577	-700541	**885281**	**-849752**
Fres	**411556**	**433430**	**744585**	**748746**	**981301**	**938515**
Mx [Nm]	-3620	-3738	-9949	-10086	**-9192**	**-8273**
Mz [Nm]	116	86	1578	1426	**2212**	**2550**
angle [°]	50	50	70	69	**65**	**65**

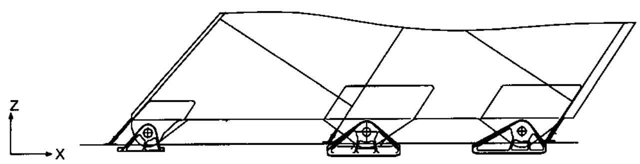

Figure 4.2

Table 4.2 **Lateral Load Yokes Reaction Forces**

	Front [N]		Centre [N]		Rear [N]	
	LHS	**RHS**	**LHS**	**RHS**	**LHS**	**RHS**
Fx	-1404	1332	-1229	1134	-8616	9387
Fy	18894	17934	16797	15510	70787	77127
Fz	-1598	1517	-1872	1728	-13146	14324
Fres	**19013**	**18047**	**16946**	**15647**	**72511**	**79005**

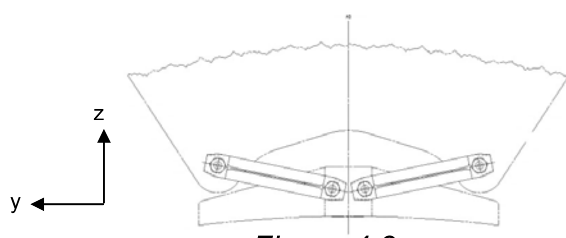

Figure 4.3

Bonding conditions *Cond I & II* are described in chapter 3.6.

4.3 Fitting forces of W375 bonding *Cond II* [NASTRAN / linear static]

Rudder deflection angle	[°]	-11,47

Table 4.3 **Main Fitting Reaction Forces**

Embedded 3D rear main lug

	Front [N]		Centre [N]		Rear [N]	
	LHS	**RHS**	**LHS**	**RHS**	**LHS**	**RHS**
Fx	267186	-281946	257989	-274238	**413562**	**-392218**
Fy	9174	9463	31200	31897	**49859**	**37726**
Fz	321498	-336976	710085	-715335	**871777**	**-845717**
Fres	418131	439472	756143	766765	**966186**	**933003**
Mx [Nm]	-3677	-3790	-10116	-10309	**-9135**	**-7368**
Mz [Nm]	124	91	1632	1471	**2108**	**1539**
angle [°]	50	50	70	69	**65**	**65**

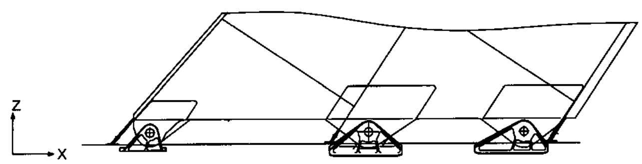

Figure 4.4

Table 4.4 **Lateral Load Yokes Reaction Forces**

	Front [N]		Centre [N]		Rear [N]	
	LHS	**RHS**	**LHS**	**RHS**	**LHS**	**RHS**
Fx	-1390	1319	-1251	1193	-9637	9900
Fy	18708	17752	17101	16310	79177	81335
Fz	-1582	1501	-1905	1817	-14704	15105
Fres	**18826**	**17864**	**17252**	**16454**	**81106**	**83316**

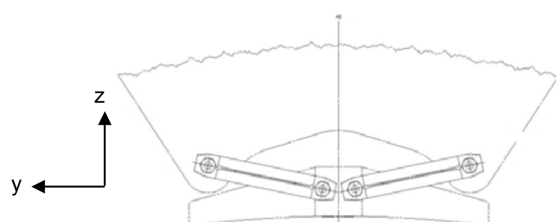

Figure 4.5

Bonding conditions *Cond I & II* are described in chapter 3.6.

4.4 Comparison of NASTRAN RHS rear main fitting forces [absolute values / linear static]

The 180°-degree bonding (as described in chapter 3.6) is the best approach to model the contact situation. Regarding the forces the bonding condition (see diagram 4.1) has the most influence on the lateral force Fy, which decrease about 20%. In the main directions Fx and Fz the decrease of load was negligible. The influence of the bonding condition on the local lug moments (see diagram 4.2) leads to a decrease of 40% to 60% and corresponds better with the ANSYS nonlinear contact analysis.

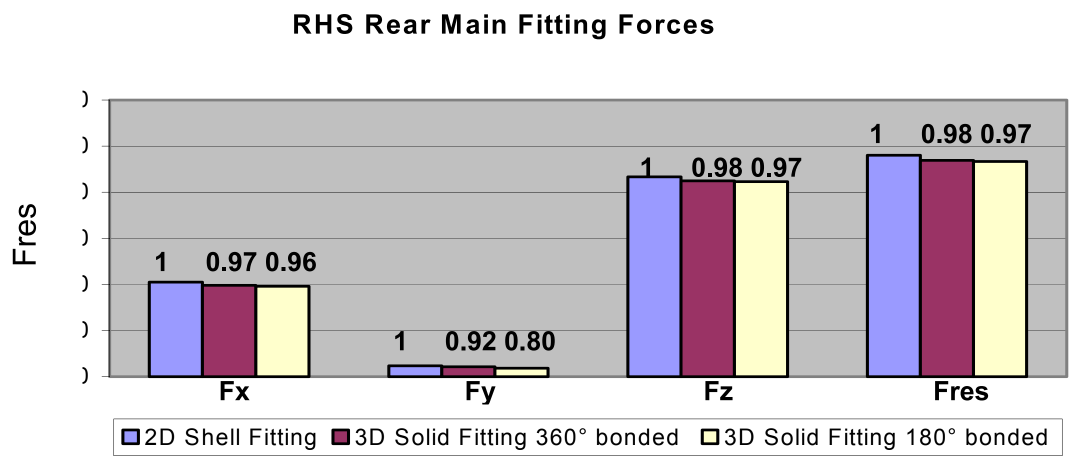

Diagram 4.1

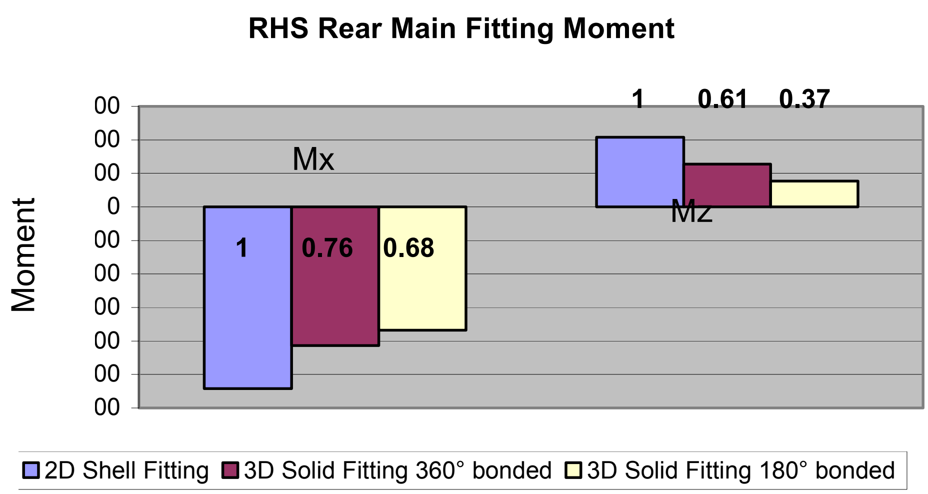

Diagram 4.2

4.5 Bonding *Cond I and II* differences in deformations

Figure 4.6 to 4.9 show the differences in the deformation behaviour of the fin / fuselage connection area for the RHS rear main lug under W375 load case (tension side).

Cond I

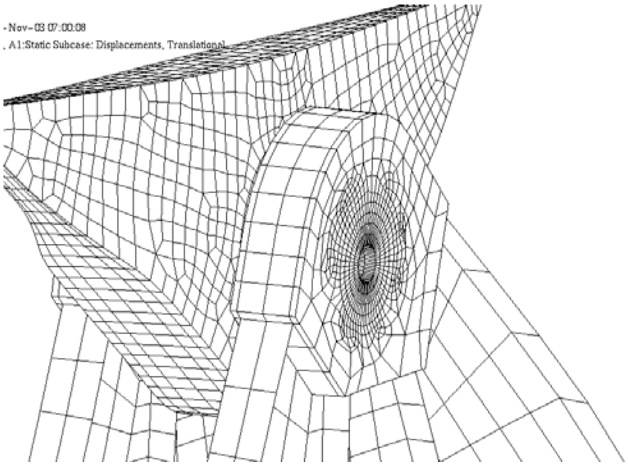

Figure 4.6

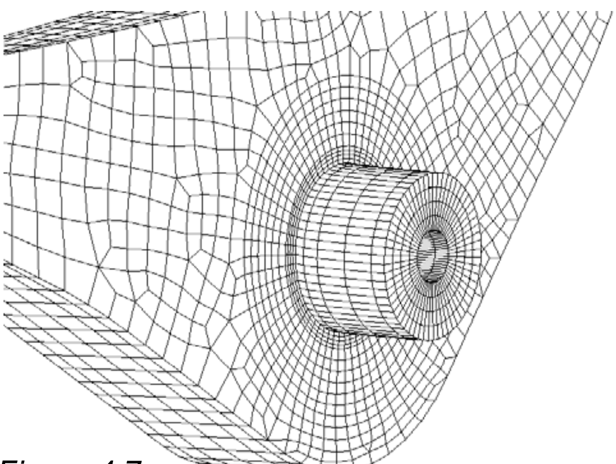

Figure 4.7

Cond II

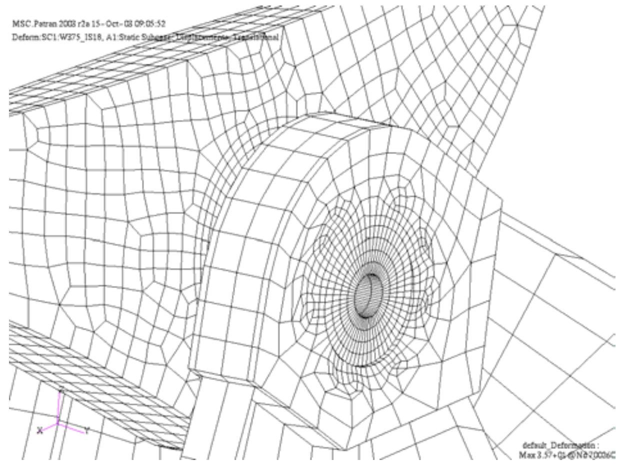

Figure 4.8

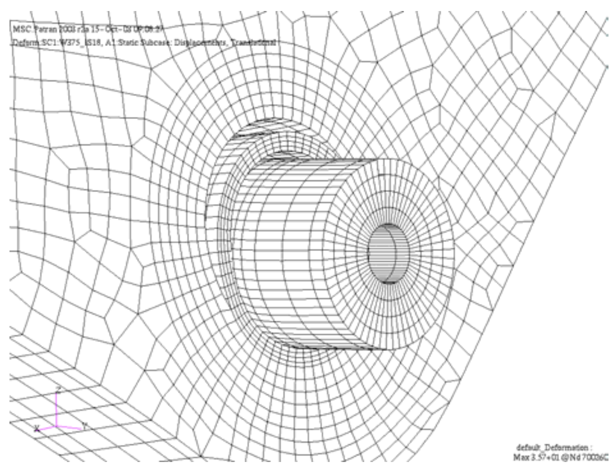

Figure 4.9

Deformations are scaled up for a better understanding of the structure behaviour

4.6 Rear main fitting forces for design gust case BI17 [NASTRAN / linear static / *Cond II* / scaled to full scale test Fres level]

The full scale rupture test in 1986 was performed with the design gust loading condition and a structural temperature of 70°C (ΔT=+50K).
The structure failed at the RHS rear main lug under tension load.

The tension load vector at the **rear main fitting** at failure was:

Table 4.5

Component		Force
Fx	[kN]	-289
Fy	[kN]	-38
Fz	[kN]	-854.8
Fres	[kN]	902.34

The analysis of the global model with the embedded rear lugs gives the following attachment forces on the tension side (no temperature effect):

Table 4.6

Component		Force
Fx	[kN]	-171
Fy	[kN]	19
Fz	[kN]	-424
Fres	[kN]	458

Considering the 50K temperature differential and a limit load factor of 2 on the gust case BI17 the RHS rear main fitting force results in:

Table 4.7

Component		Force
Fx	[kN]	-281
Fy	[kN]	37
Fz	[kN]	-853
Fres	[kN]	899

Bonding Condition ***Cond II***

Table 4.8 **Main Fitting Reaction Forces**

Embedded 3D rear main lug

	Front [N]		Centre [N]		Rear [N]	
	LHS	RHS	LHS	RHS	LHS	RHS
Fx	215000	-326000	218000	-235000	**405855**	**-281334**
Fy	10900	16400	26600	38700	**38321**	**36805**
Fz	367000	-373000	744000	-728000	**838975**	**-853287**
Fres	**425480**	**495655**	**775737**	**765968**	**932773**	**899223**
Mx [Nm]	-3840	-4700	-10400	-10900	**-8080**	**-8120**
Mz [Nm]	230	-53	1540	1250	**1671**	**1557**
angle [°]	60	49	74	72	**64**	**72**

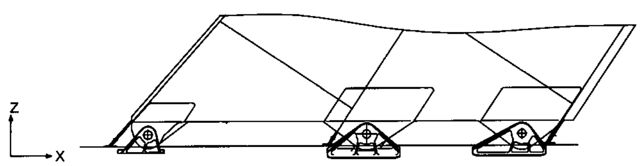

Figure 4.10

Table 4.9 **Lateral Load Yokes Reaction Forces**

	Front [N]		Centre [N]		Rear [N]	
	LHS	RHS	LHS	RHS	LHS	RHS
Fx	-2520	2830	-1750	2420	-5100	8180
Fy	33900	38100	24000	33100	41900	67200
Fz	-2870	3220	-2670	3690	-7780	12500
Fres	**34114**	**38340**	**24211**	**33393**	**42920**	**68840**

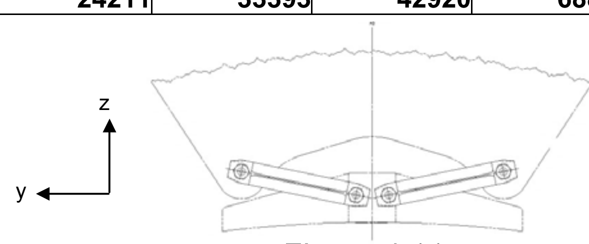

Figure 4.11

5. Boundary displacements for ANSYS RHS contact 3D model

The global NASTRAN 2D model with the embedded LHS & RHS 3D models was analyzed with accident loading W375 and delivers the displacement boundary conditions for the RHS ANSYS contact 3D model and a set of main fitting forces (see figure 5.1).

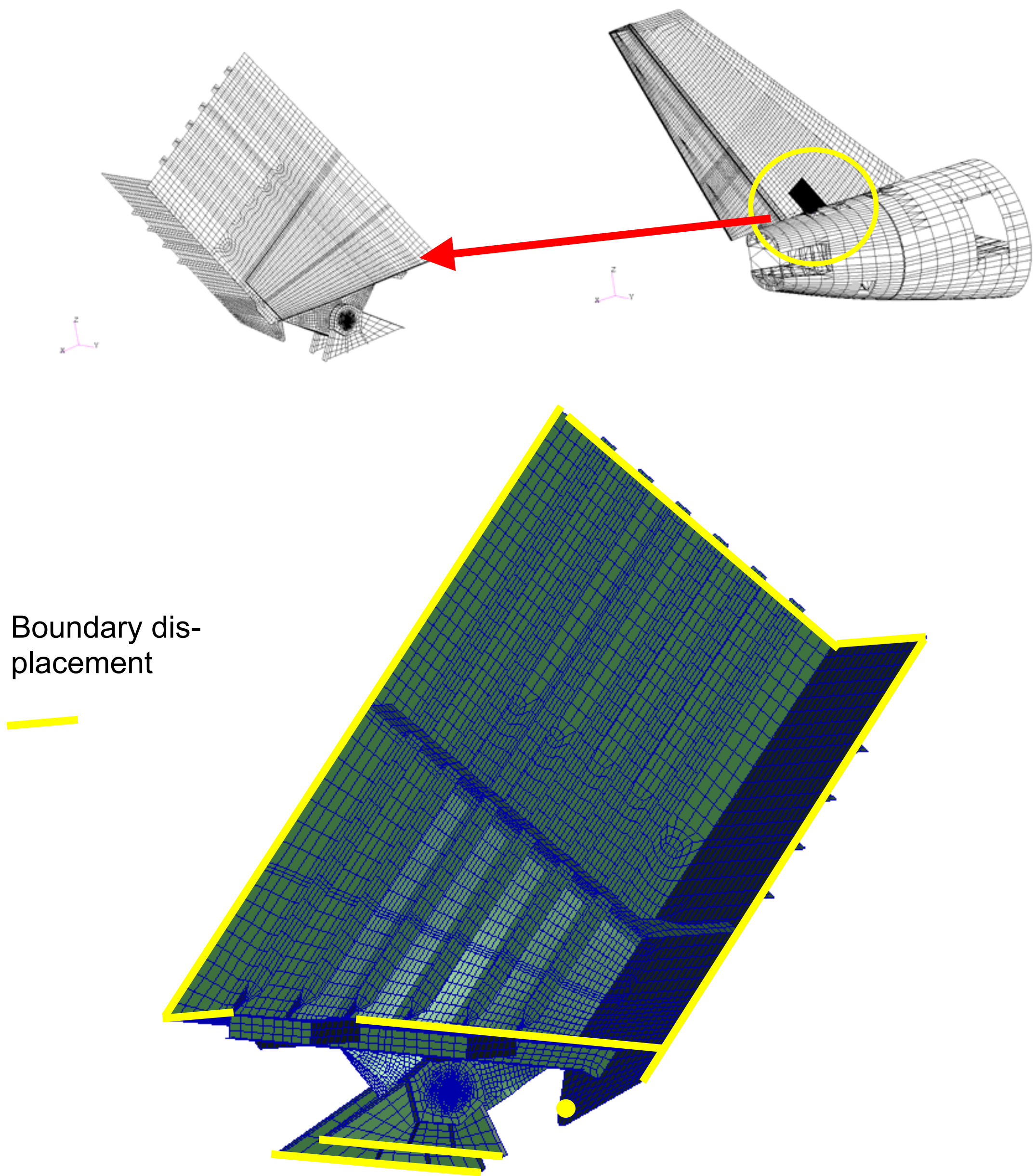

Figure 5.1

During the model development process several comparisons were made between the NASTRAN and the ANSYS model to validate that under the same analysis conditions the results are within acceptable tolerances. A linear static analysis was performed with the same bonded lug and boundary displacement conditions. The result of the main fitting forces of both models were in agreement.

In the next step the RHS ANSYS contact 3D model was loaded with these displacement boundary conditions.
The performed ANSYS FE-Analysis is a geometric nonlinear contact analysis. The displacements were applied in several steps. For each step the local fitting reactions are calculated.

The resulting main fitting force of the RHS ANSYS nonlinear contact analysis under W375 loading conditions was Fres=856kN. This indicates as expected, that the contact model has a lower stiffness than the embedded 3D model with partially bonded pin.

The Airbus approach is to scale the ANSYS resultant force to the level of the NASTRAN resultant vector. (See report "*AAL587 Airbus Structure Investigation – FEM Global to Local analysis details*" TN – ESGC – 1019/03).

Scale factor for the boundary displacements

$$Scale_{RHS} = \frac{Fres\_W375\_MOD}{Fres\_RHS\_ANSYS\_Contact} = \frac{933kN}{856kN} = 1{,}09$$

For the comparison with the NASA W375 MOD load vector, the boundary displacement conditions were scaled up with a factor of 1.09. It is valid to scale the displacements, because the global deformation of the VTP follows a linear behavior. The ANSYS RHS contact analysis, with the scaled up boundary displacement set, results in a main fitting resultant force of Fres=936kN.

6. ANSYS RHS 3D model

The figure 6.1 and 6.2 show the RHS 3D nonlinear contact model, which was used for the detailed lug reaction and strain distribution analysis.

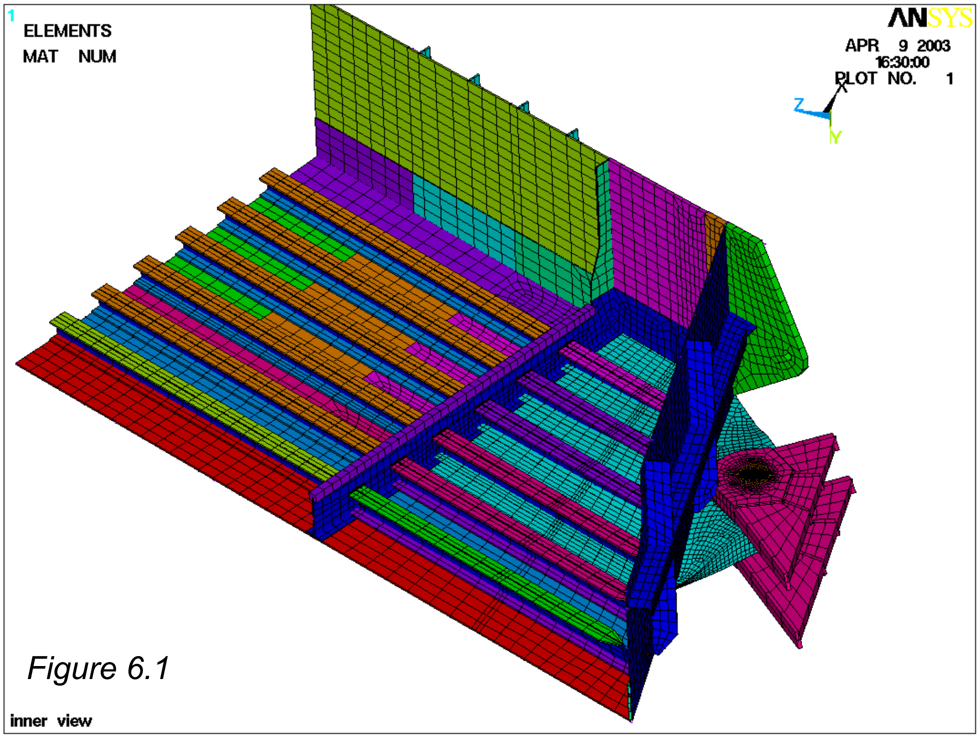

Figure 6.1

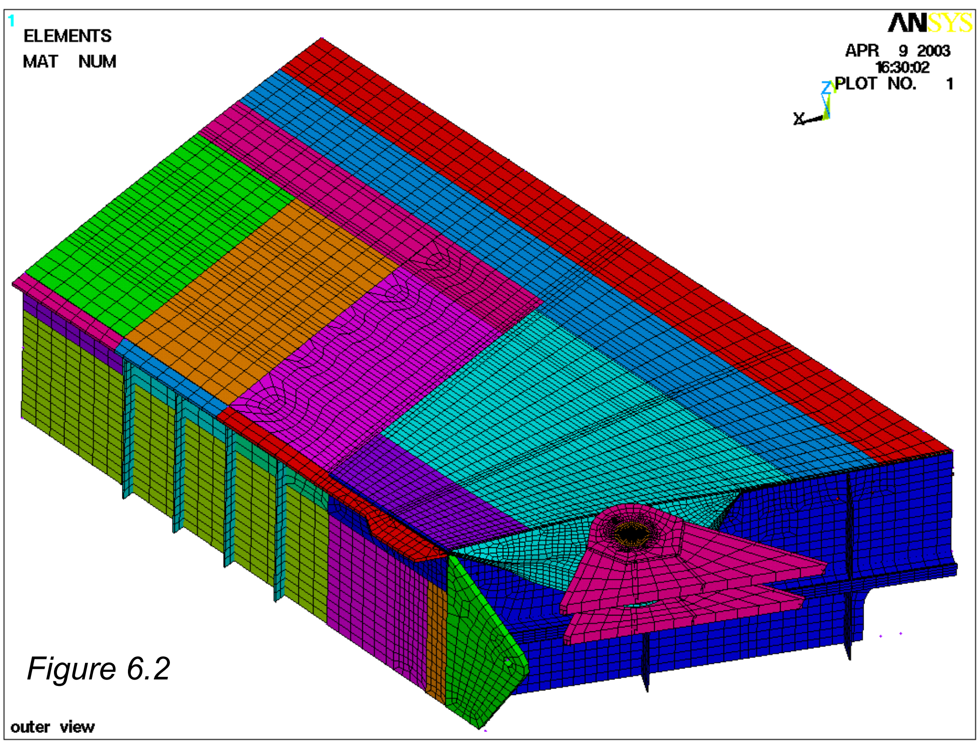

Figure 6.2

6.1 ANSYS Contact surface definition

The contact surface definitions are the same for all ANSYS models (see figure 6.3 to 6.6). The ANSYS contact surface allows physically opening and closing gaps between the meshes of the contact borders with a friction coefficient of 0.3.

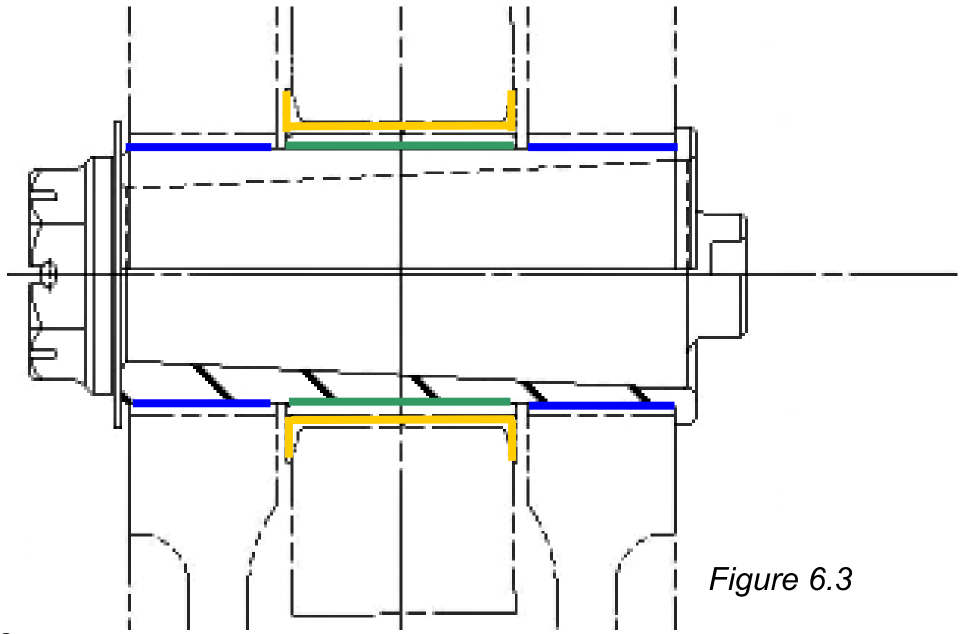

Figure 6.3

<u>Contact surfaces:</u>

Bushing to CFRP lug surface **Fuselage clevis to bolt surface** **Bolt to bushing surface**

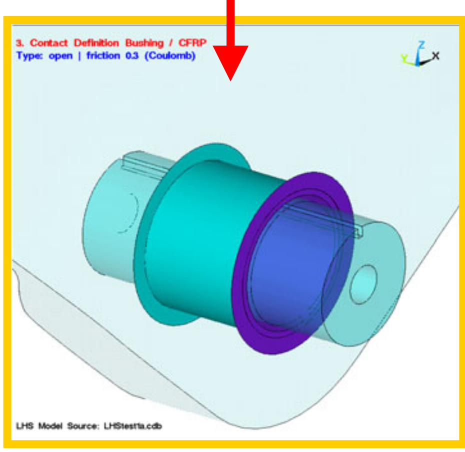

Figure 6.4

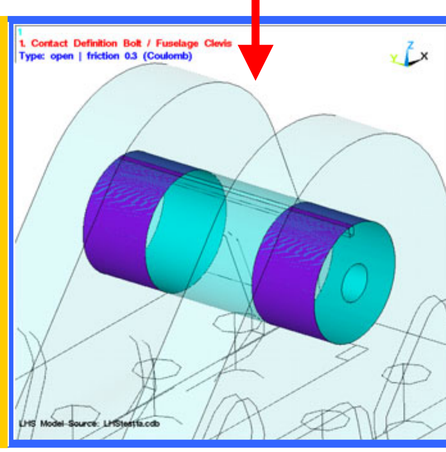

Figure 6.5

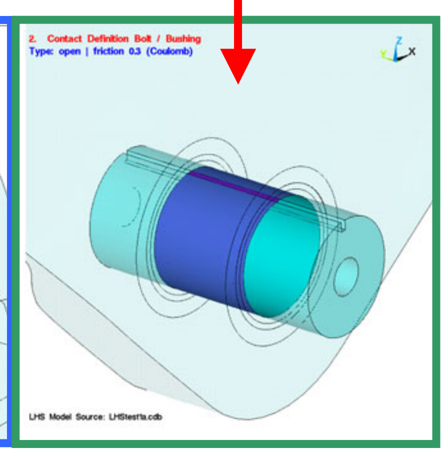

Figure 6.6

6.2 Lug reaction force & moment calculation in ANSYS [nonlinear contact]

The local lug reactions are calculated in the ANSYS model for every load step. At a defined cut through the fuselage clevis (see figure 6.7) the summation of the grid point force balance in this cut gives the local lug reaction including respective forces & moments. Also the deformation of the complete bolt area is taken into account for this procedure.

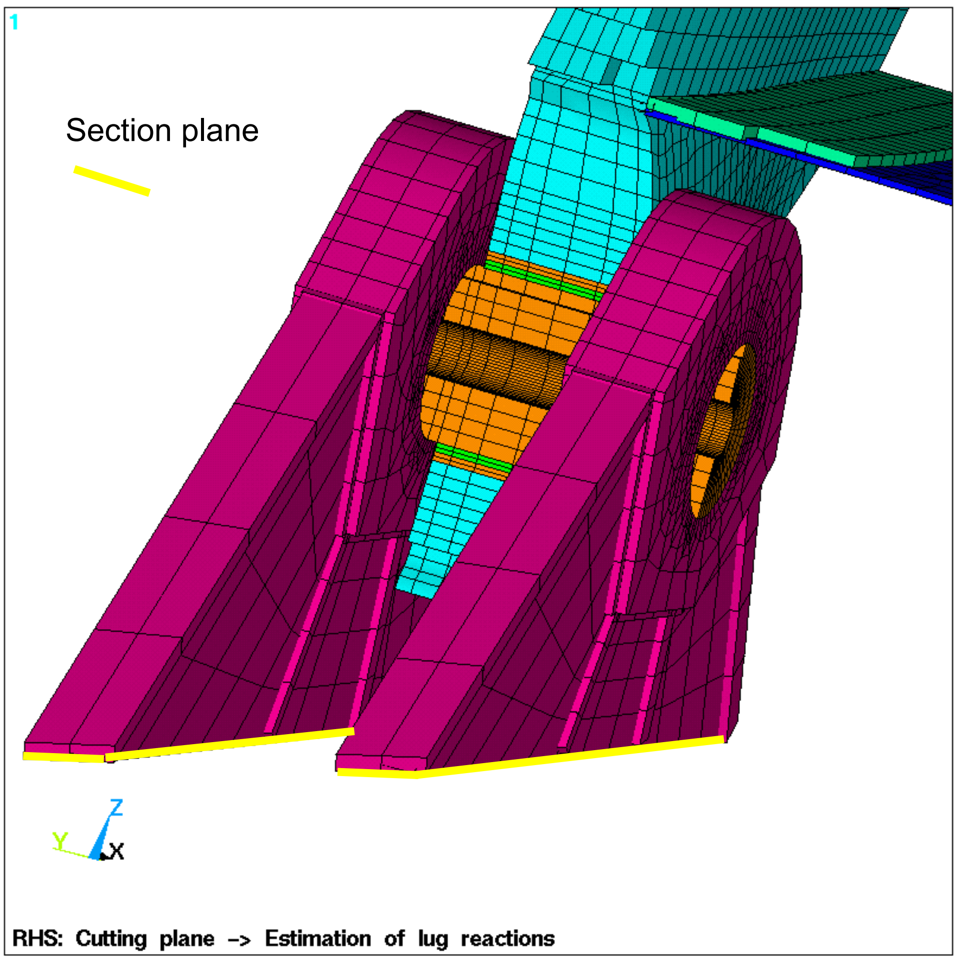

Figure 6.7

The calculation of bolt rotation and lug reactions on displaced lug center was made with user written subroutine in ANSYS (APDL).

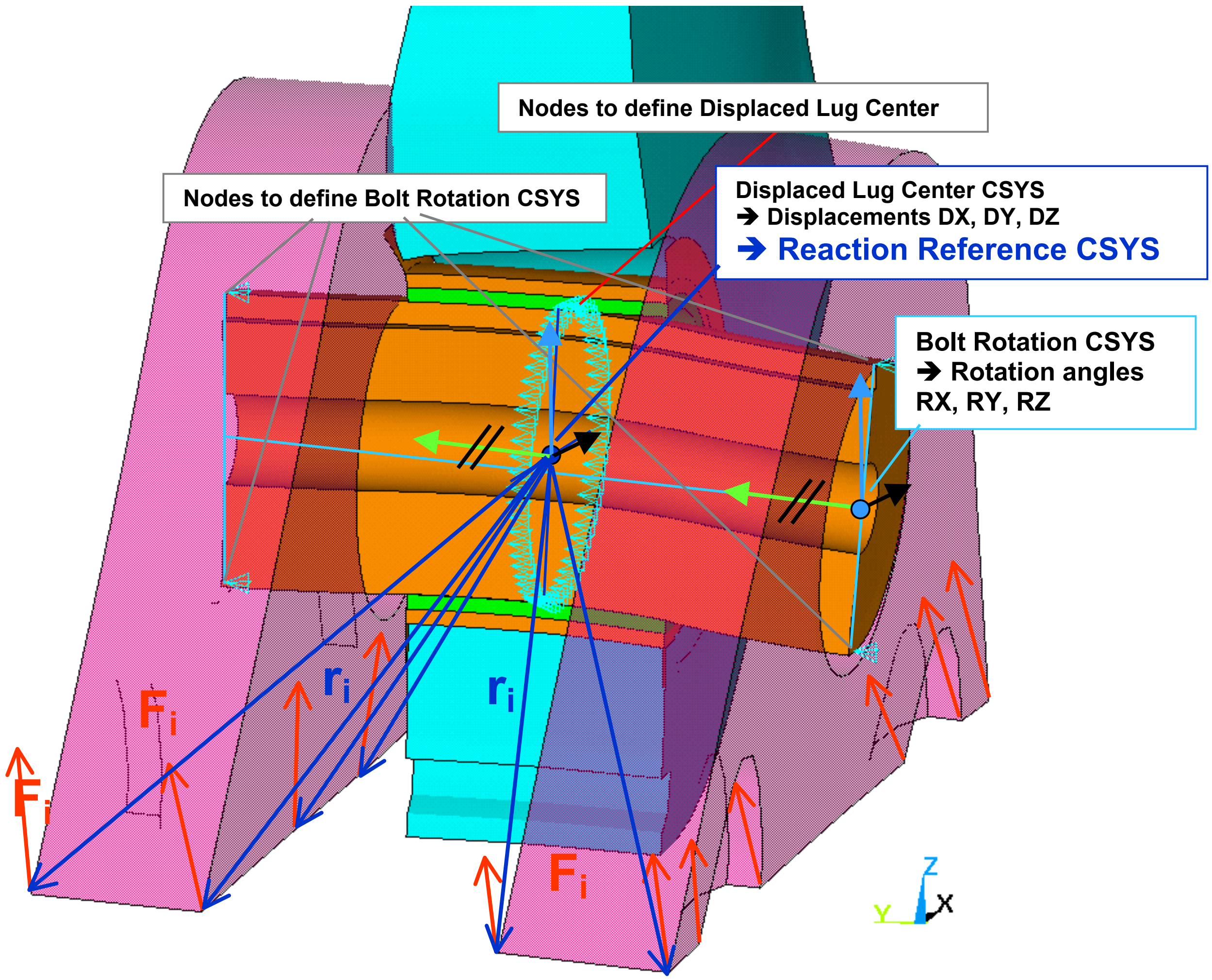

Deformed structure! (Displacements scaled by a factor 10)

➔ Reactions in Displaced Lug Centre:

$$M_{RsP} = SUM(r_i \times F_i) \qquad F_{RsP} = SUM(F_i)$$

Figure 6.8

6.3 ANSYS method to calculate the Rx bolt rotation relative to the displaced rib 1

The figure 6.9 describes the ANSYS method for the calculation of bolt displacements and rotation relative to rib 1.

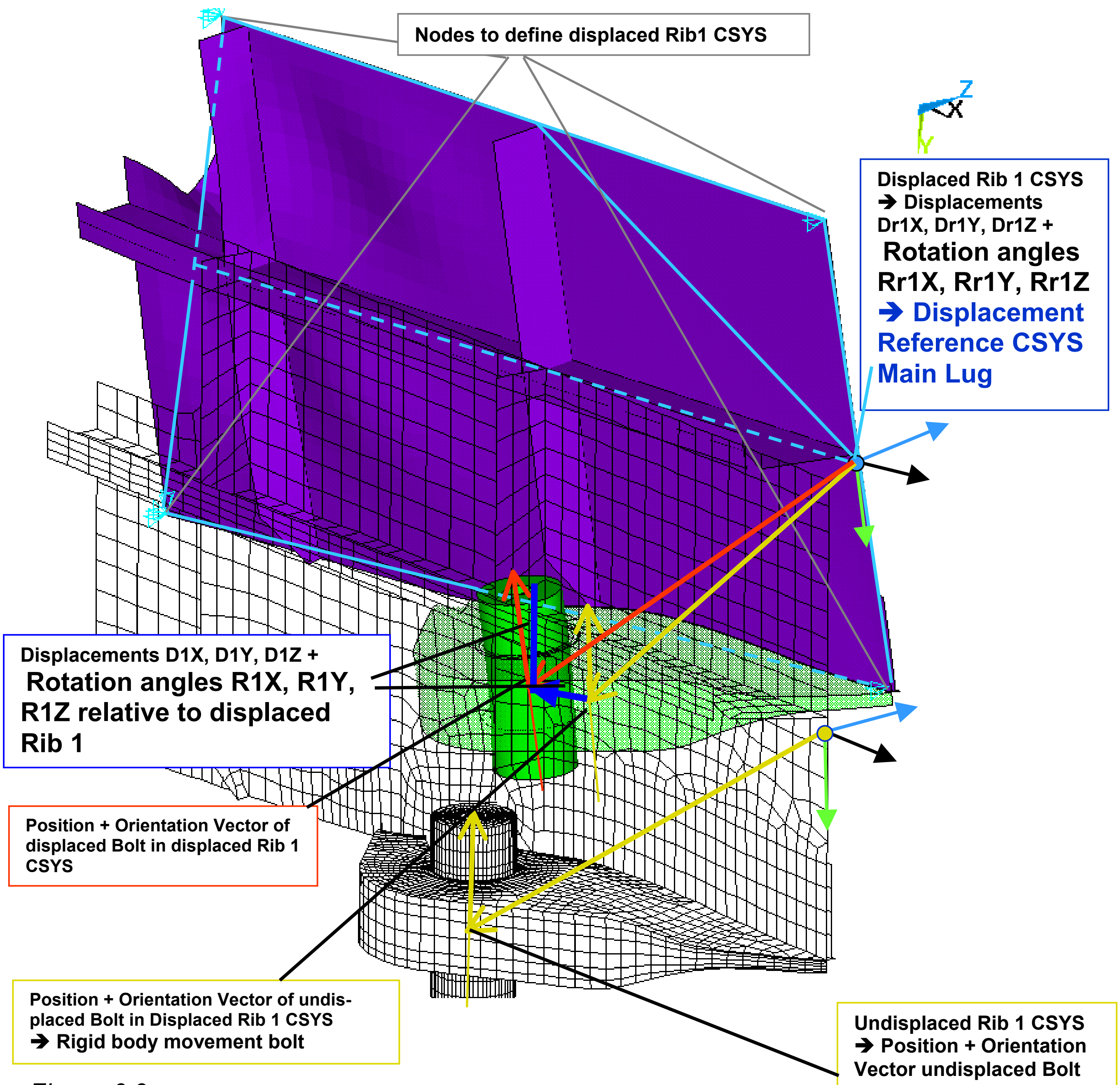

Figure 6.9

7. ANSYS results

7.1 RHS ANSYS contact 3D model W375 [scaled on NASTRAN Fres level]

7.1.1 RHS rear main local lug forces & moments

Table 7.1

Fx [kN]	Fy [kN]	Fz [kN]	Fres [kN]	Mx [Nm]	Mz [Nm]	Rx [°]	Rz [°]
0	0	2	**2**	4	8	0	0
-63	5	-132	**146**	-1015	187	-0,073	0,014
-124	11	-264	**292**	-2042	372	-0,146	0,029
-186	18	-403	**444**	-3150	566	-0,219	0,044
-250	25	-548	**602**	-4319	747	-0,292	0,059
-315	33	-698	**766**	-5542	908	-0,365	0,074
-381	42	-853	**936**	-6807	1051	-0,438	0,089

Rx/Rz bolt rotation in relation to rib 1

7.1.2 Deformation & bolt Rx rotation

The cross section through the CFRP lug, the bolt and the fuselage fitting illustrates the connection bolt contact situation under max. applied loading condition. The color scale is von Mises equivalent stress distribution.

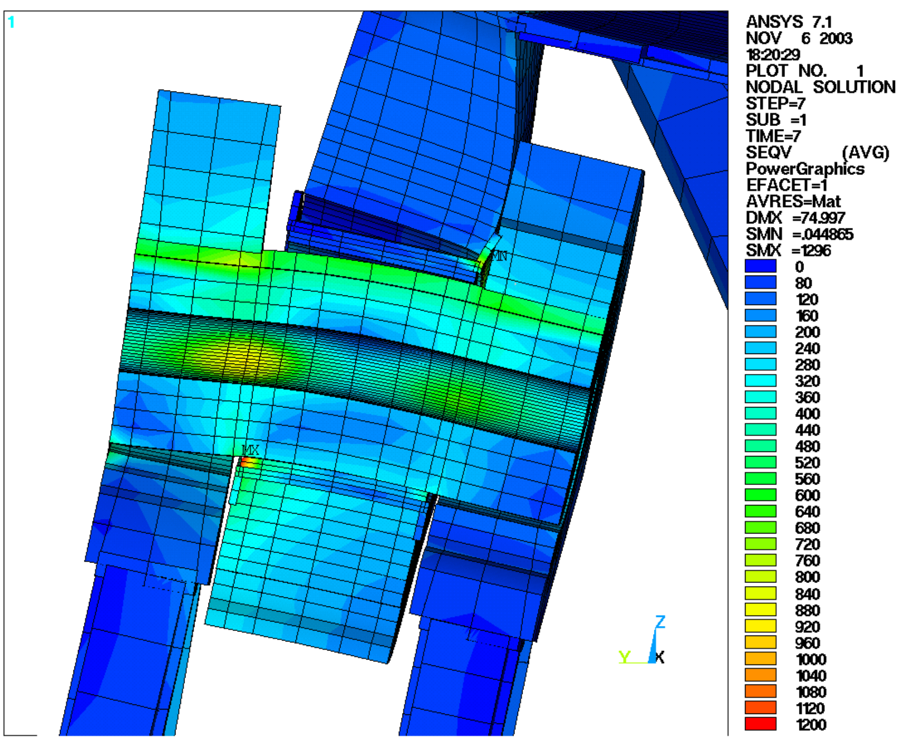

[N/mm²]

Figure 7.1

Deformations are scaled up for a better understanding of the structure behaviour

Bolt Rx rotation

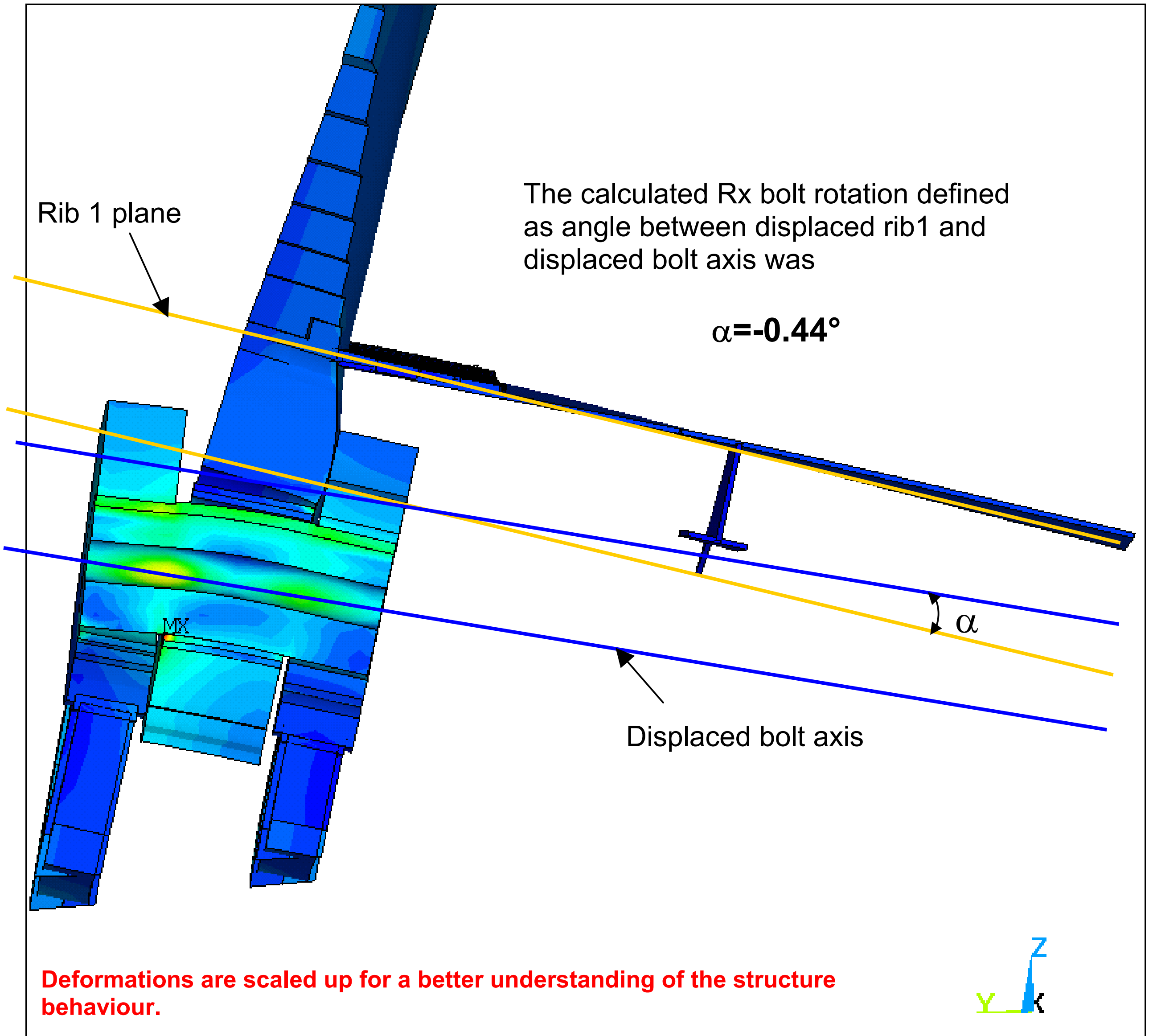

Figure 7.2

7.1.3 Contact status and pressure

Contact surface between:	Bushing & CFRP Lug

Contact status

- red + green => contact
- blue => gap

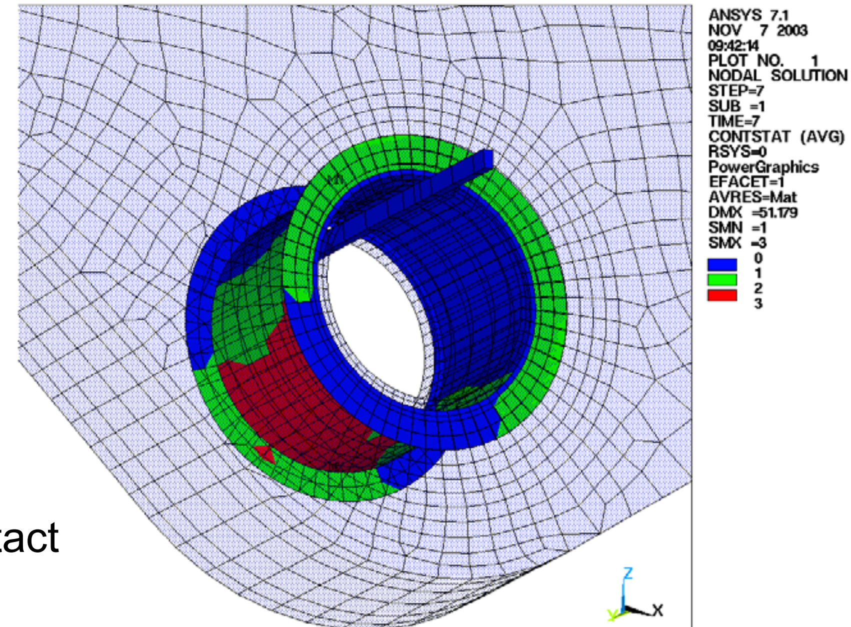

Figure 7.3

Contact pressure distribution

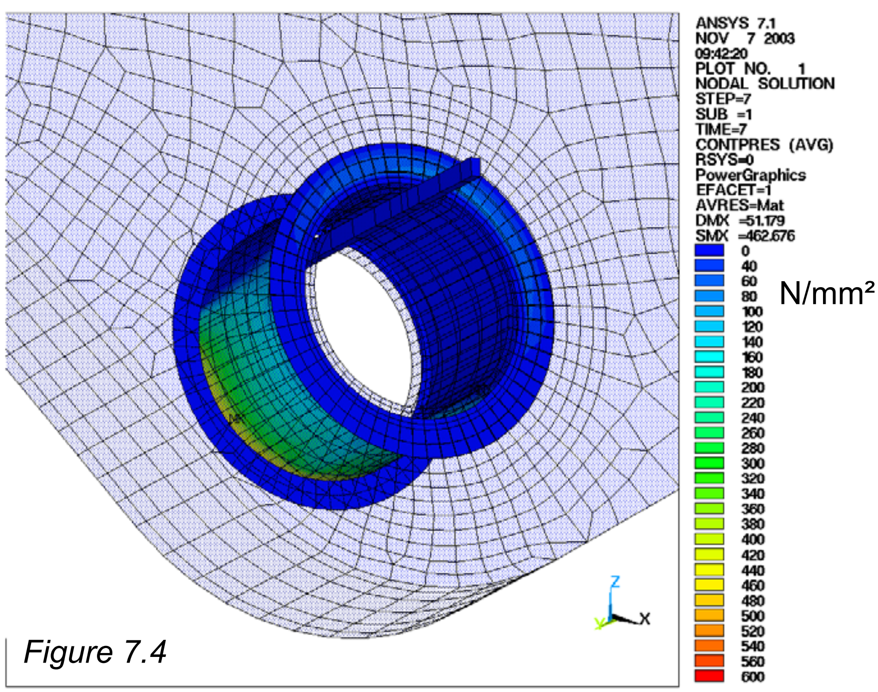

Figure 7.4

Contact surface between:	Bolt & Bushing

Contact status

- red + green => contact
- blue => gap

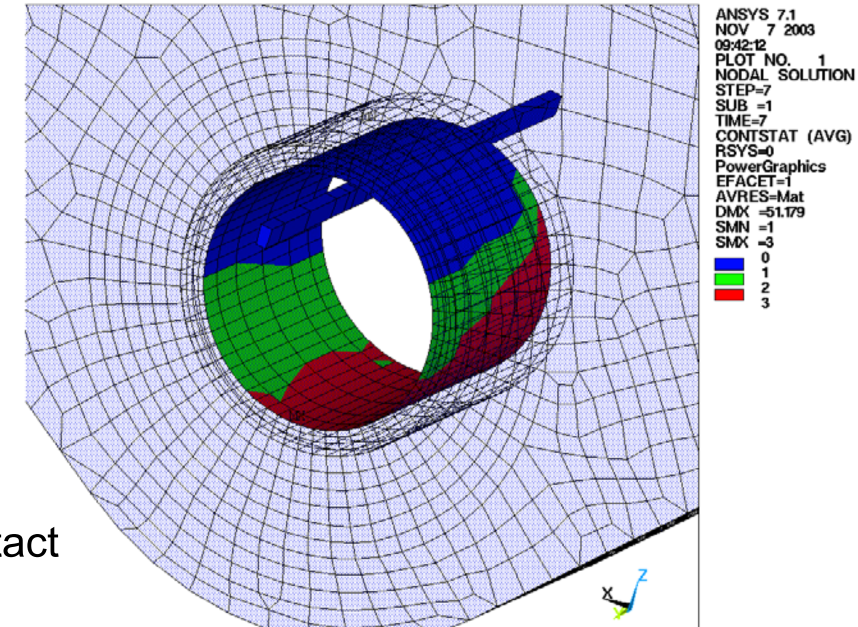

Figure 7.5

Contact pressure distribution

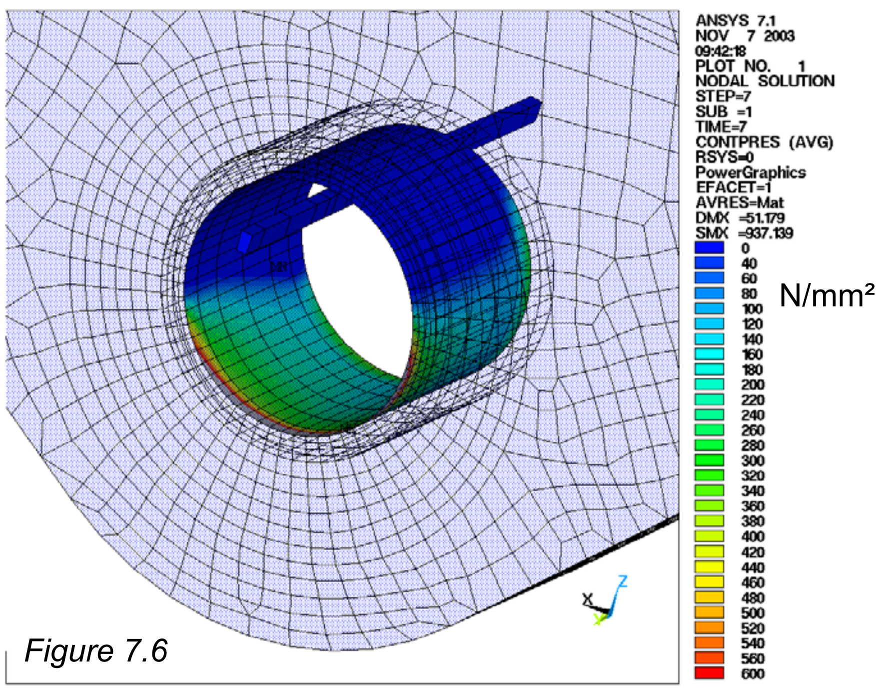

Figure 7.6

Contact surface between:	Bolt & Fuselage clevis

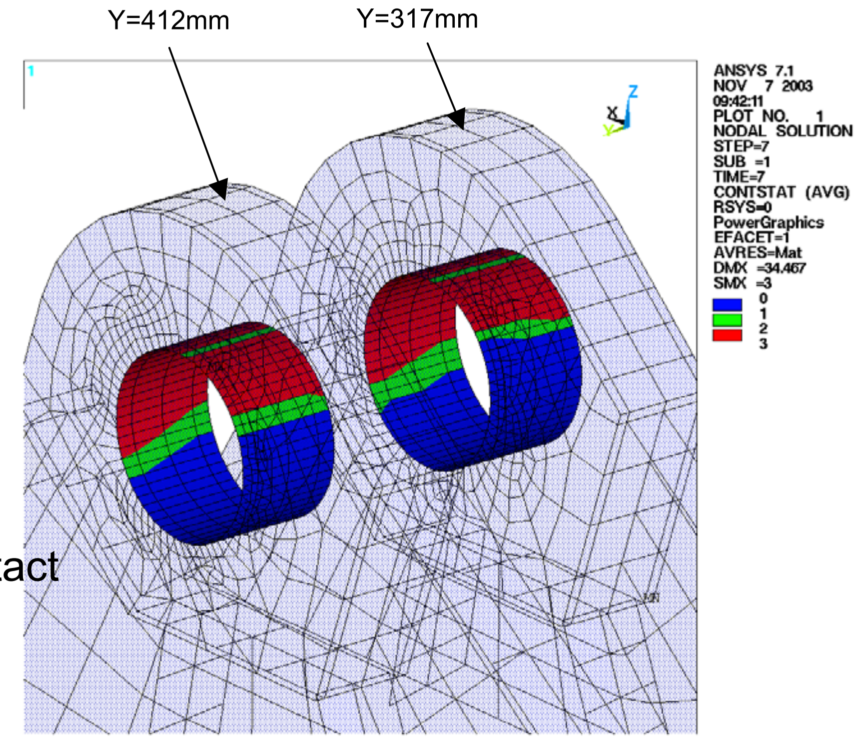

Contact status

- red + green => contact
- blue => gap

Figure 7.7

Contact pressure distribution

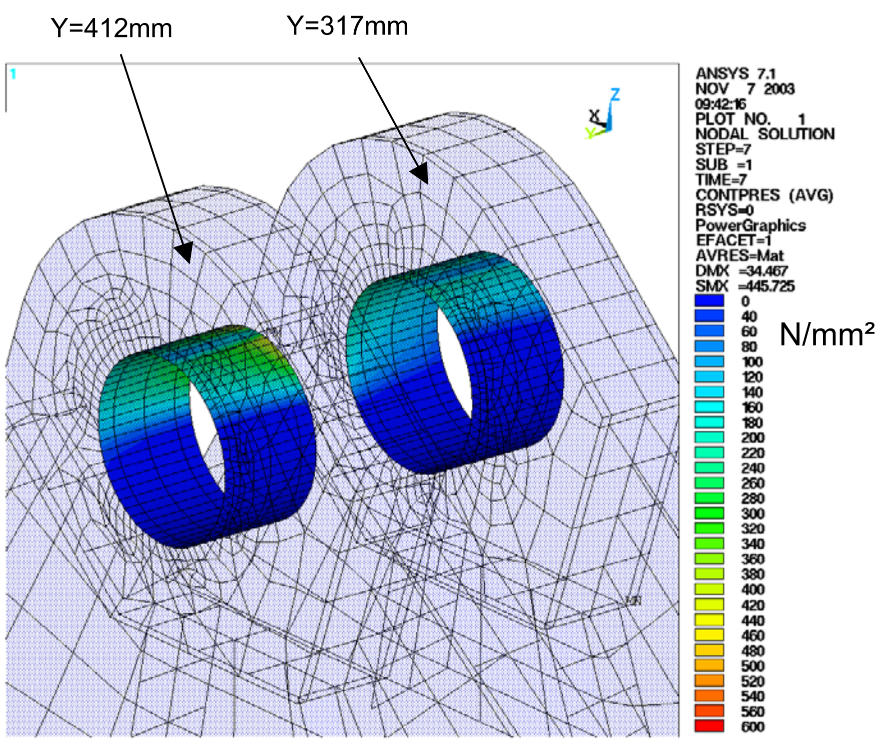

Figure 7.8

7.1.4 Strain distribution at the pin hole

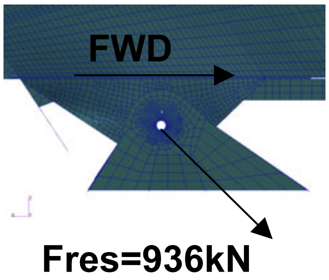

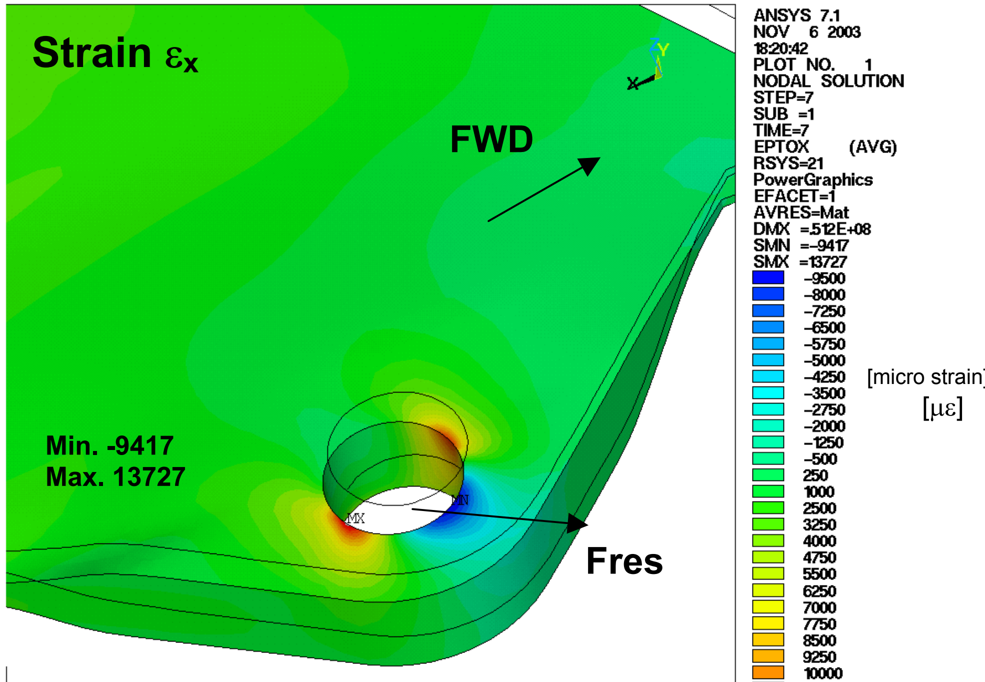

Figure 7.9

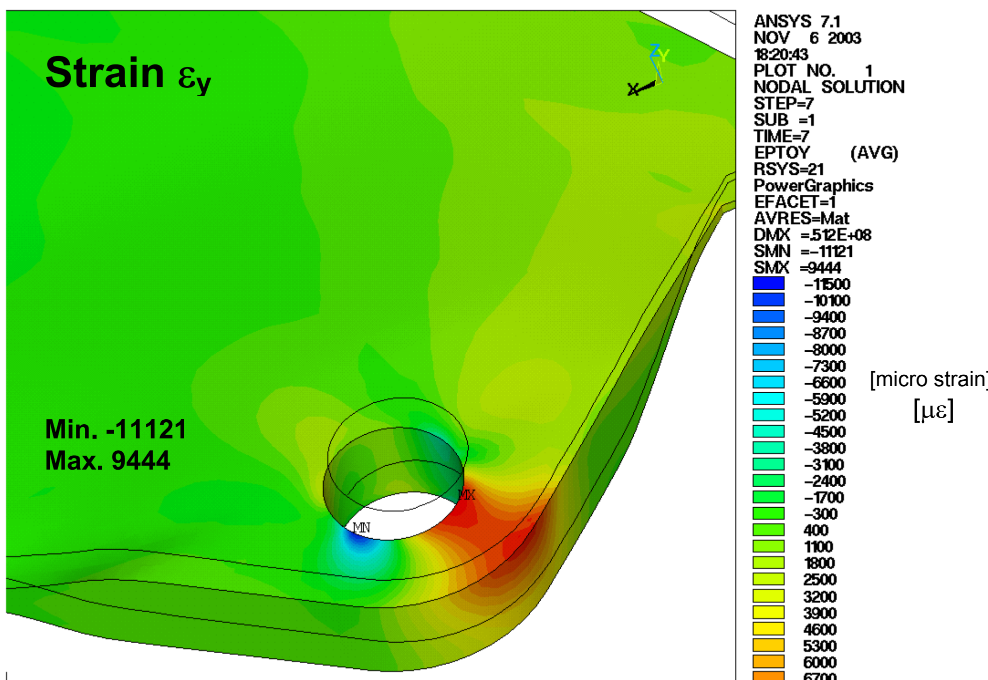

Figure 7.10

All views from outboard
Strain distribution in material coordinate system

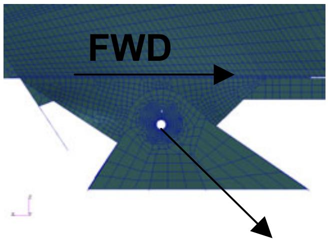

Fres=936kN

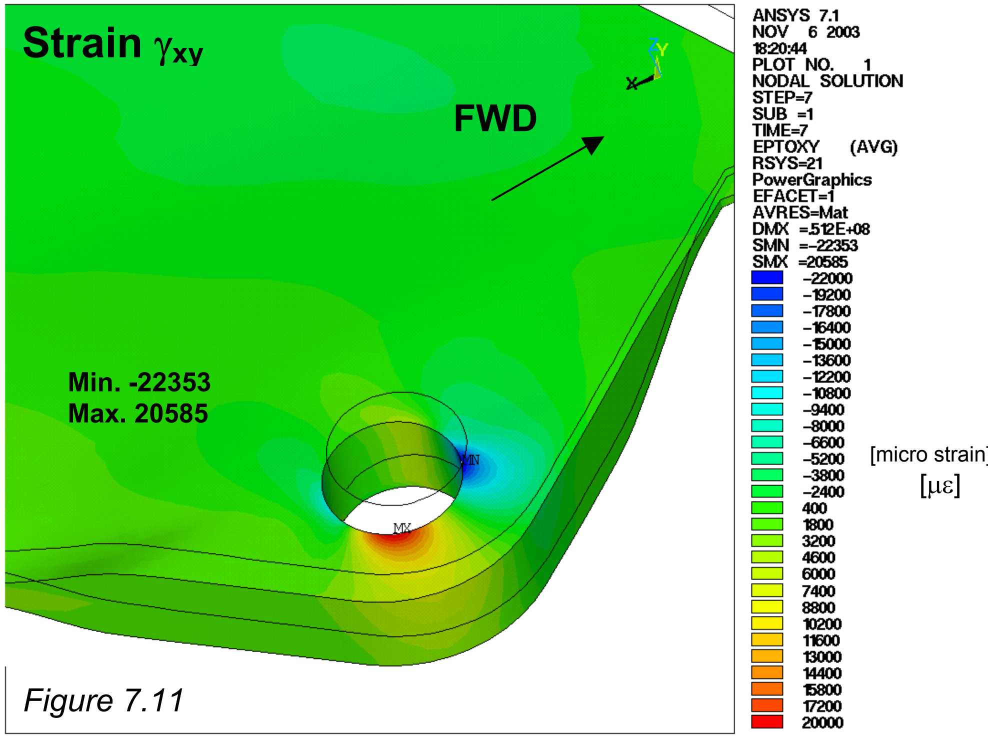

Figure 7.11

Strain$_{tangential}$
Cylinder coordinate system in the bolt axis

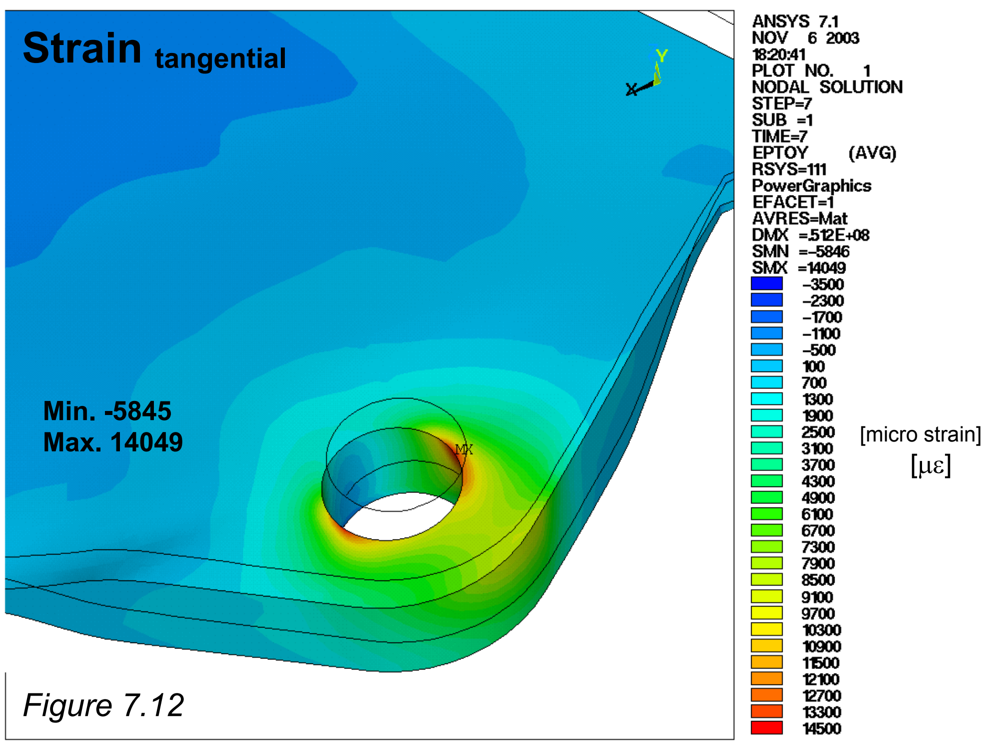

Figure 7.12

All views from outboard
Strain distribution in material coordinate system

7.2 RHS ANSYS contact 3D model design lateral gust BI17 [scaled to full scale test Fres level]

7.2.1 RHS rear main local lug forces & moments

Table 7.2

Fx [kN]	Fy [kN]	Fz [kN]	Fres [kN]	Mx [Nm]	Mz [Nm]	Rx [°]	Rz [°]
0	0	2	**2**	4	8	0	0
-52	4	-131	**140**	-925	198	-0,067	0,01
-100	7	-263	**281**	-1809	402	-0,134	0,021
-150	12	-400	**428**	-2727	624	-0,201	0,031
-201	17	-544	**580**	-3652	841	-0,269	0,042
-253	22	-694	**739**	-4574	1048	-0,337	0,053
-305	28	-849	**902**	-5482	1249	-0,405	0,064

Rx/Rz bolt rotation in relation to rib 1

7.2.2 Deformation & bolt Rx rotation

The cross section through the CFRP lug, the bolt and the fuselage fitting illustrates the connection bolt contact situation under max. applied loading condition. The color scale is von Mises equivalent stress distribution.

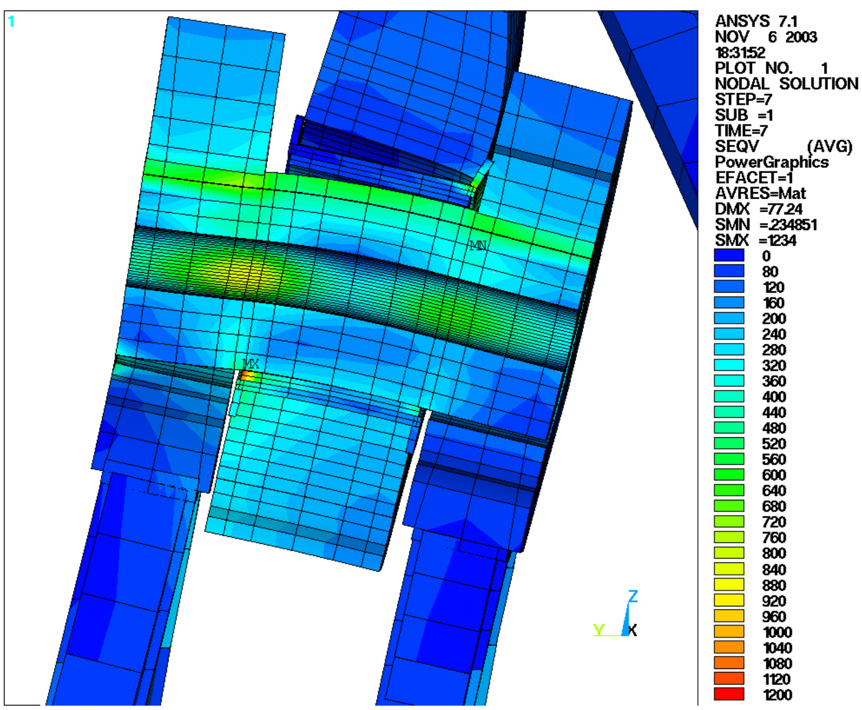

[N/mm²]

Figure 7.13

Deformations are scaled up for a better understanding of the structure behaviour

Bolt Rx rotation

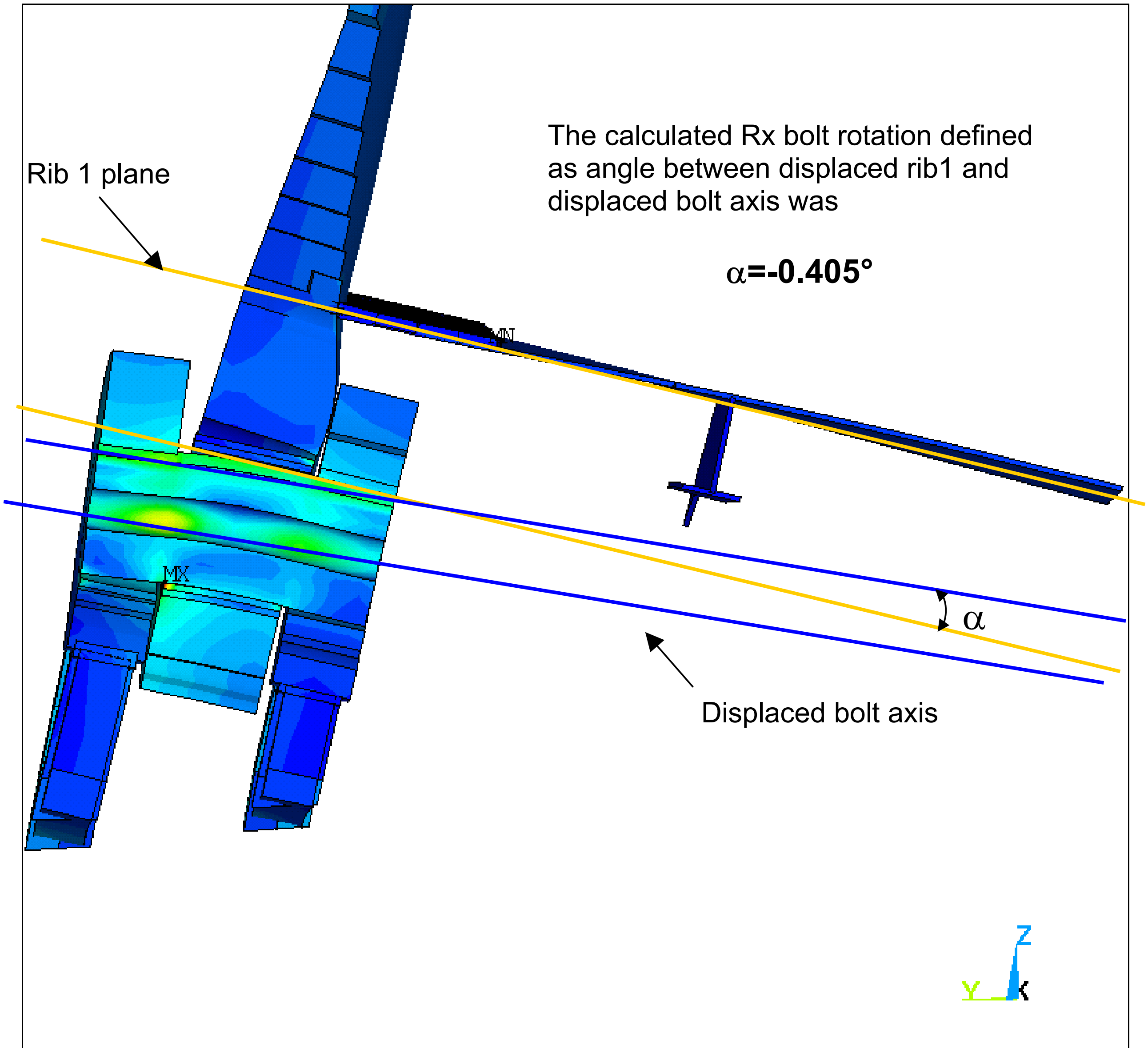

Figure 7.14

7.2.3 Contact status and pressure

Contact surface between:	Bushing & CFRP Lug

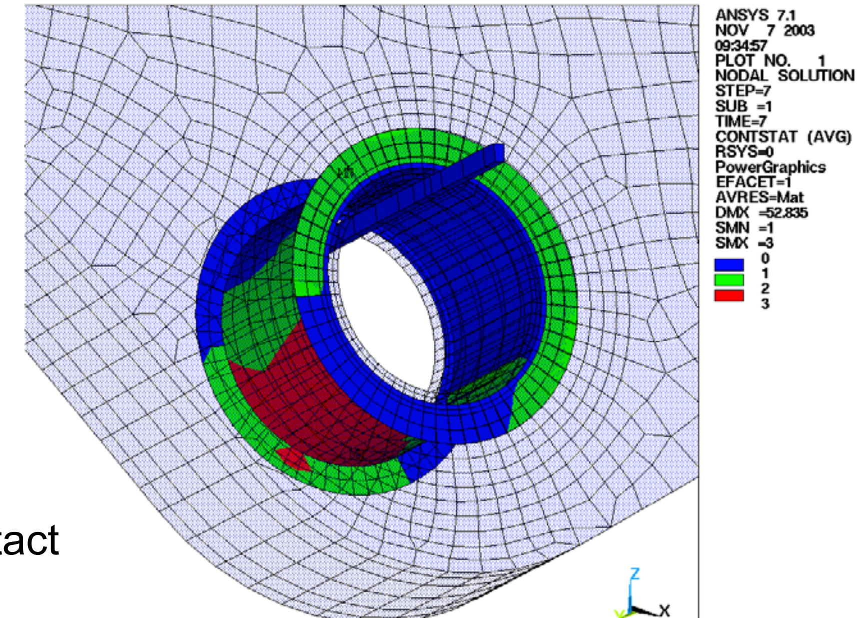

Contact status

- red + green => contact
- blue => gap

Figure 7.15

Contact pressure distribution

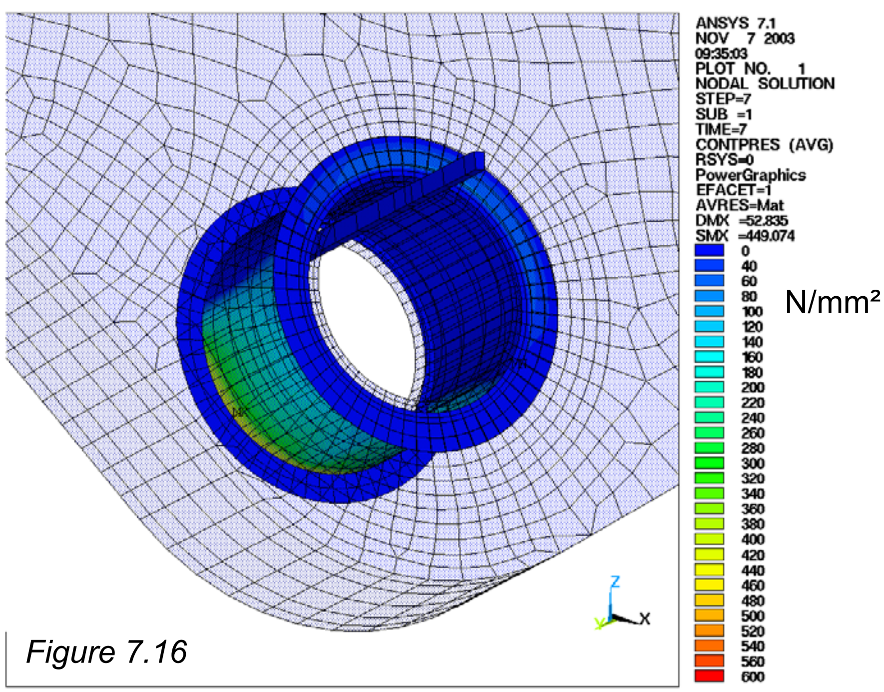

Figure 7.16

Contact surface between:	Bolt & Bushing

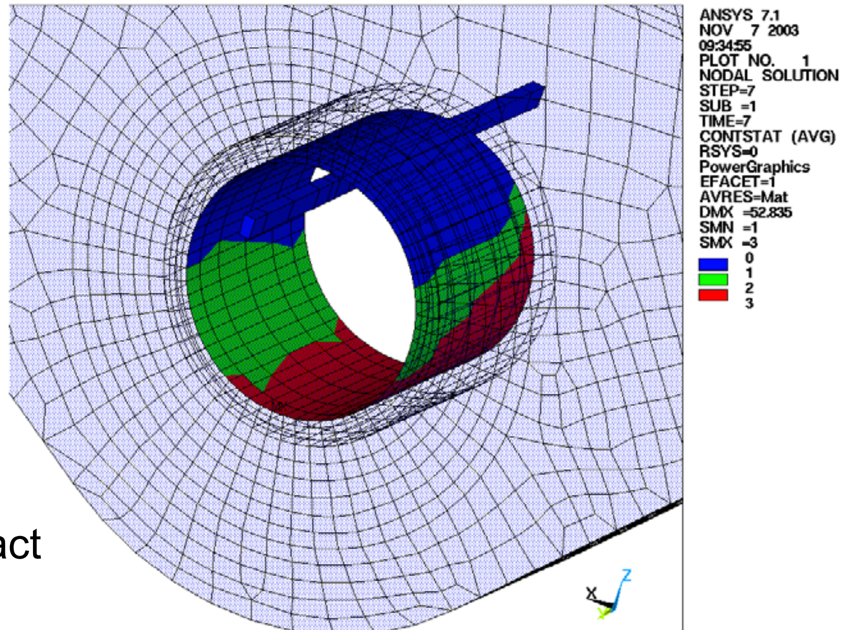

Contact status

- red + green => contact
- blue => gap

Figure 7.17

Contact pressure distribution

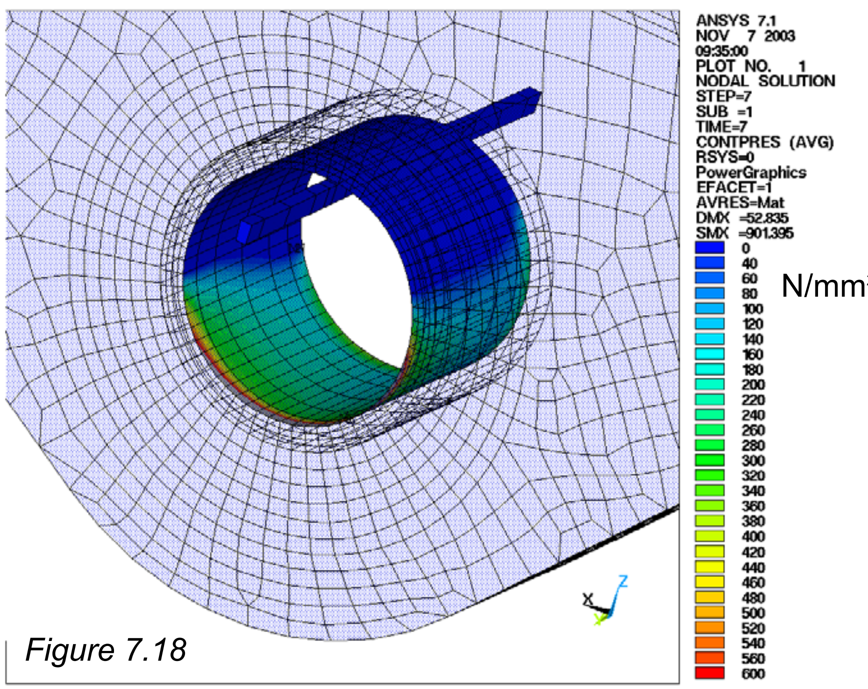

Figure 7.18

Contact surface between:	Bolt & Fuselage clevis

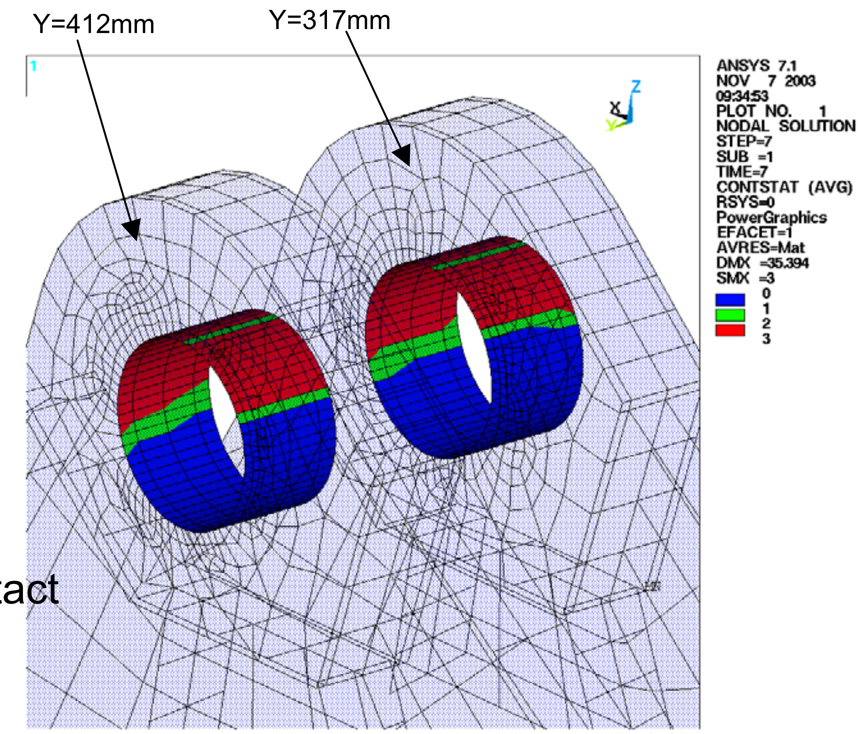

Contact status

- red + green => contact
- blue => gap

Figure 7.19

Contact pressure distribution

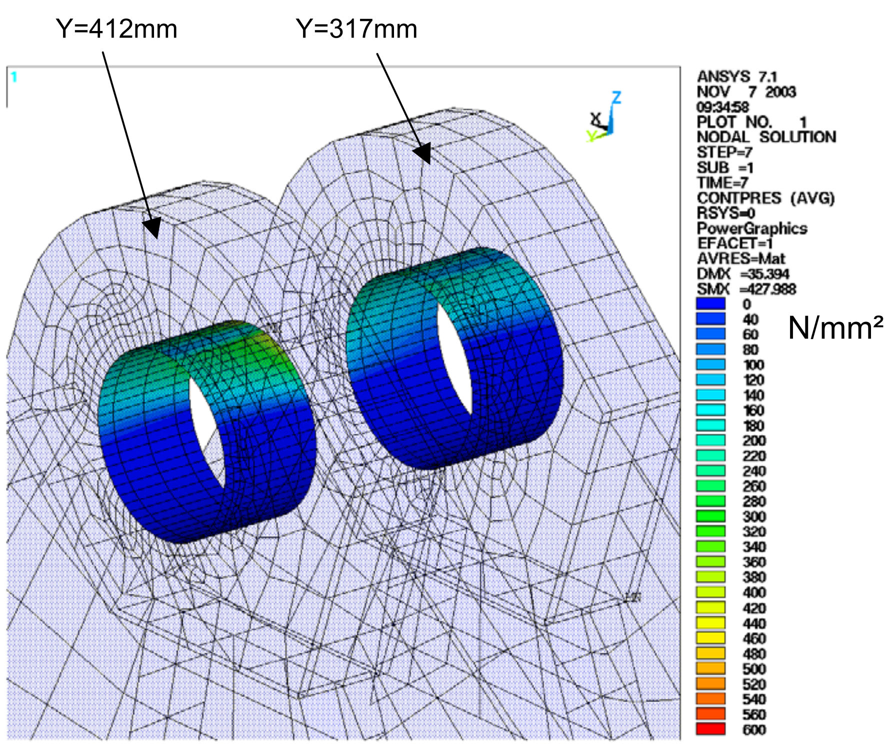

Figure 7.20

7.2.4 Strain distribution at the pin hole

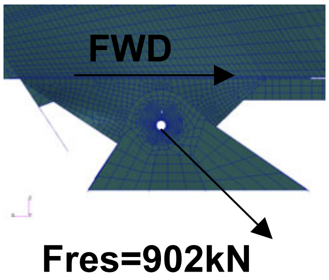

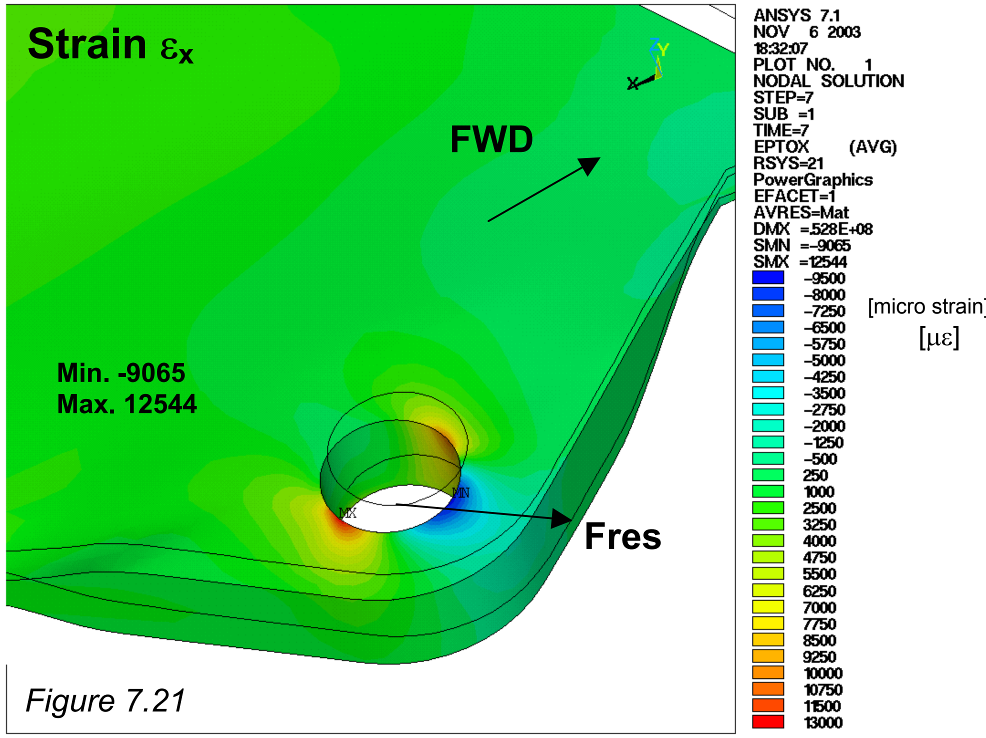

Figure 7.21

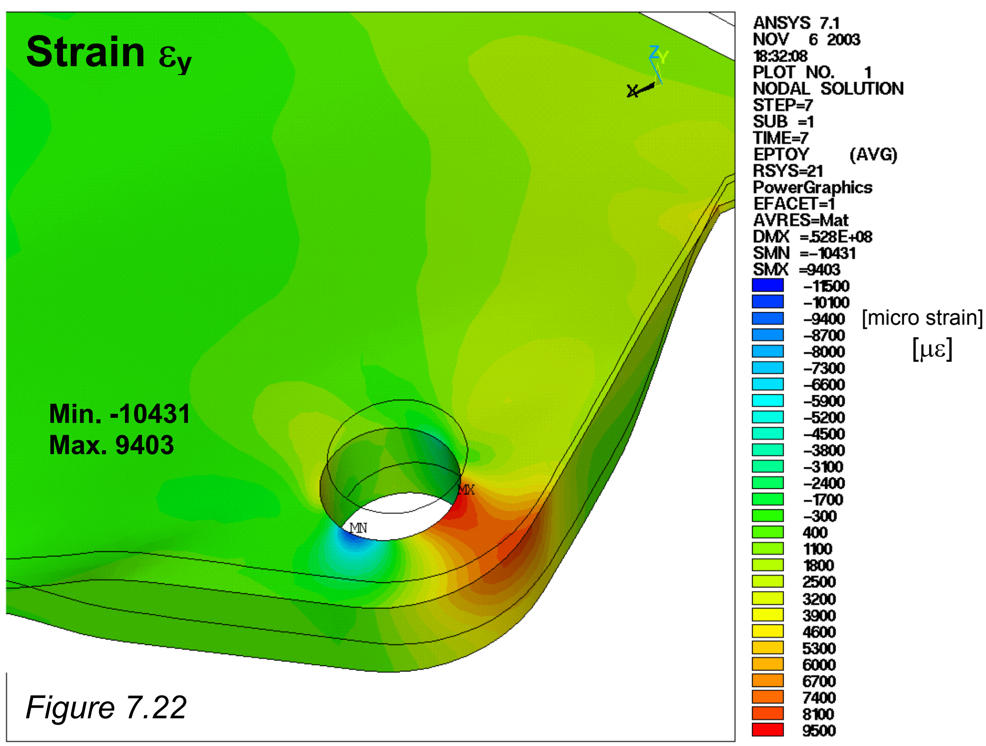

Figure 7.22

All views from outboard
Strain distribution in material coordinate system

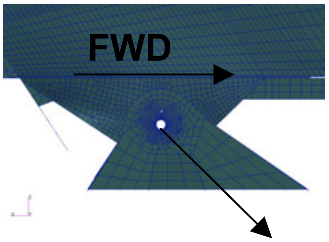

Fres=902kN

RHS model

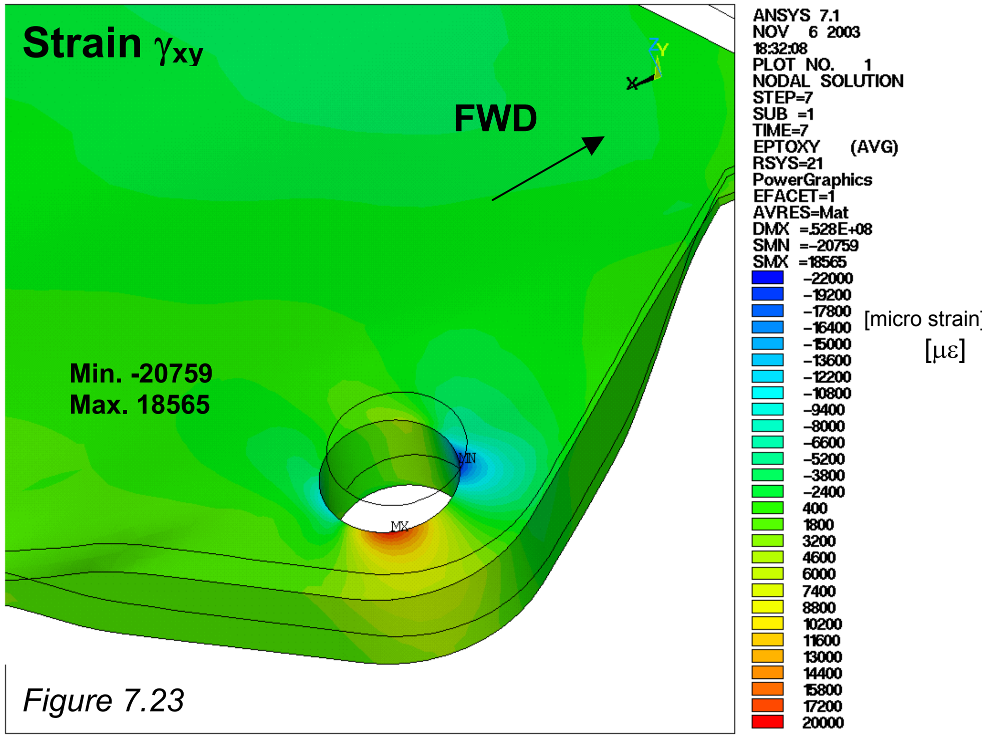

Figure 7.23

Strain$_{\textbf{tangential}}$
Cylinder coordinate system in the bolt axis

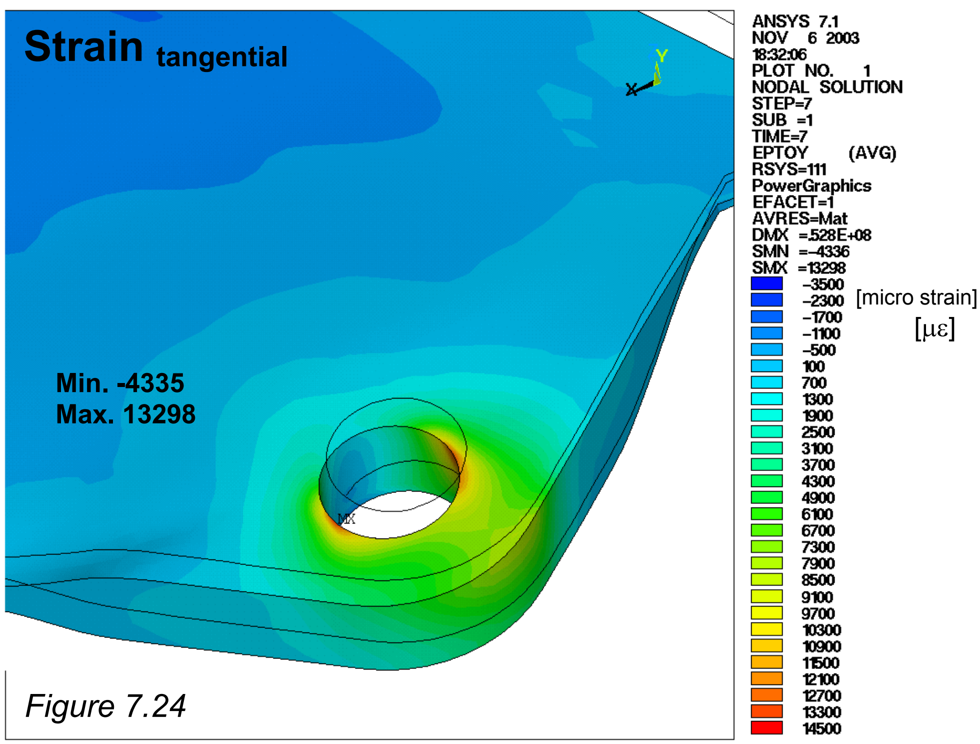

Figure 7.24

All views from outboard
Strain distribution in material coordinate system

8. Strain gauge comparison BI17 [scaled] and W375 around the lug

To enable a comparison of the BI17 [scaled] and the W375 strain distribution around the lug the same strain gauge arrangement as for the Lug Test#1 specimen was chosen. For a detailed comparison only the unidirectional strain gauges E01-E09 and the rosettes R10-R18 on both sides of the lug were selected. The discussion of the results was carried out only with the highest loaded strain gauges (see figure 8.1). These gauges are marked red in the strain gauge figure below.

Strain Gauge locations around the lug area for the BI17 and W375 comparison

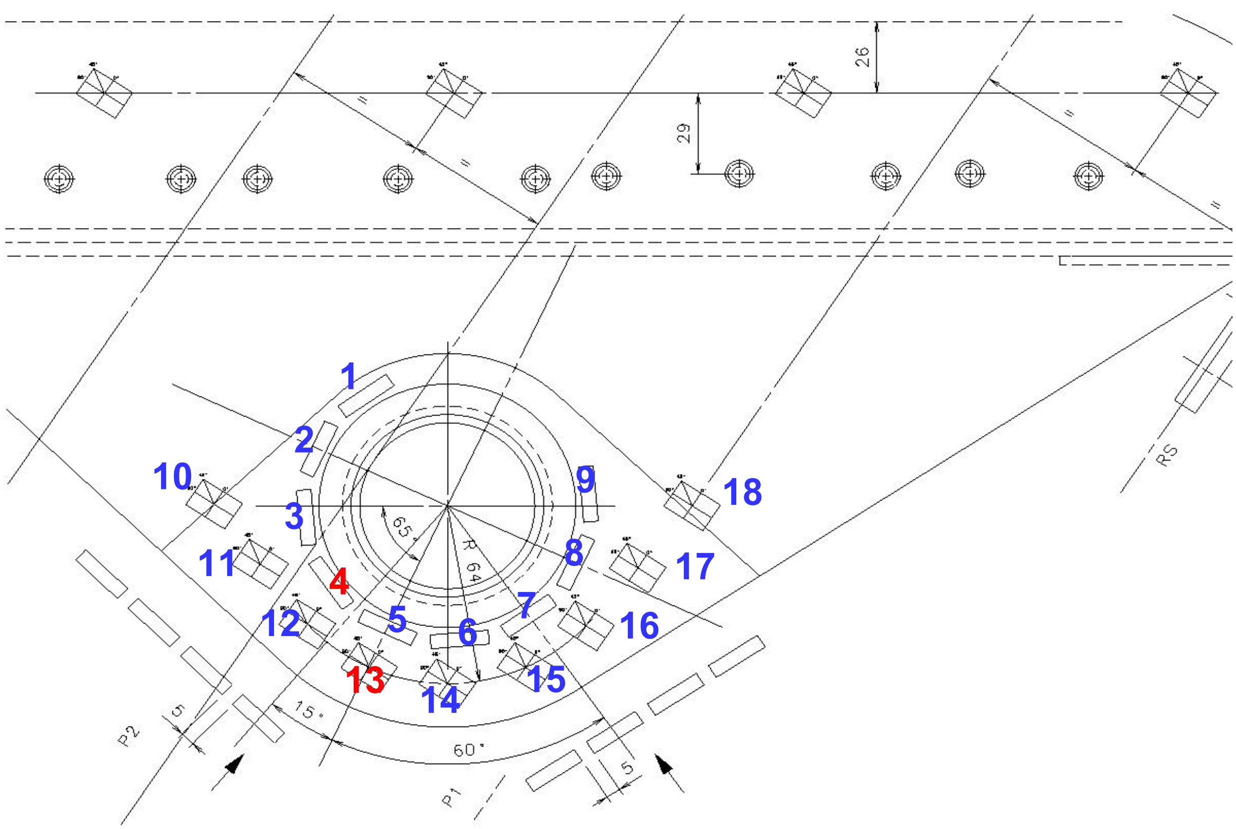

Figure 8.1

Diagram 8.1 Unidirectional Strain Gauge E04 (in- / outboard)

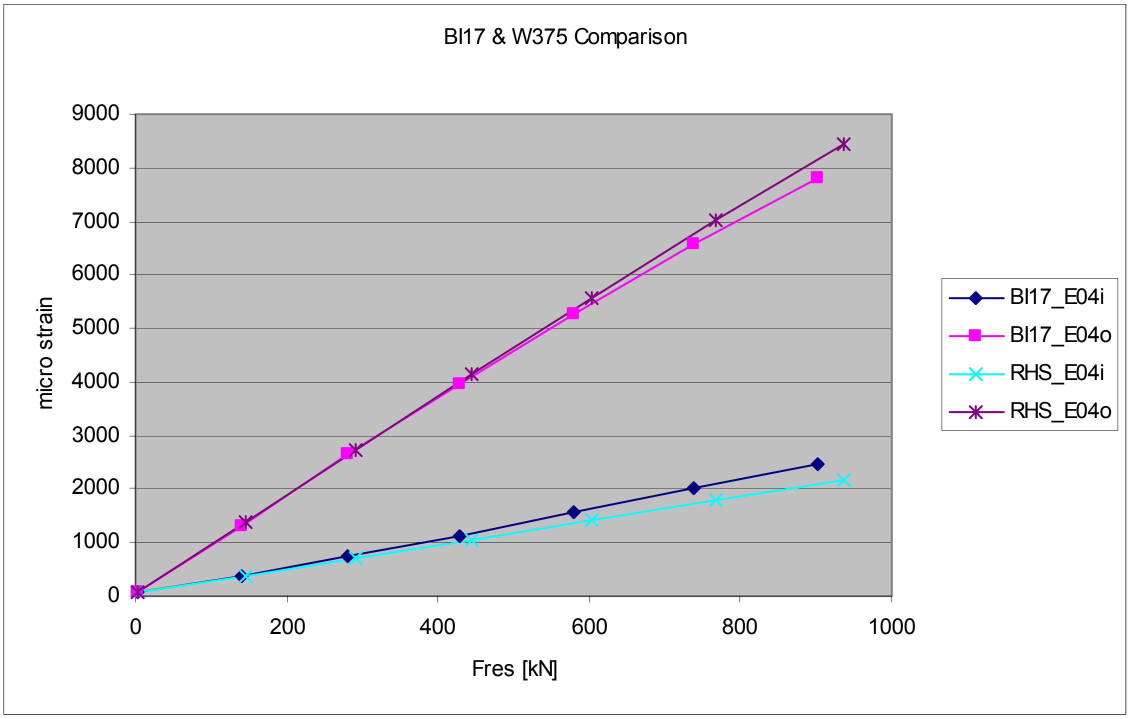

Diagram 8.2 Rosette R13o (outboard)

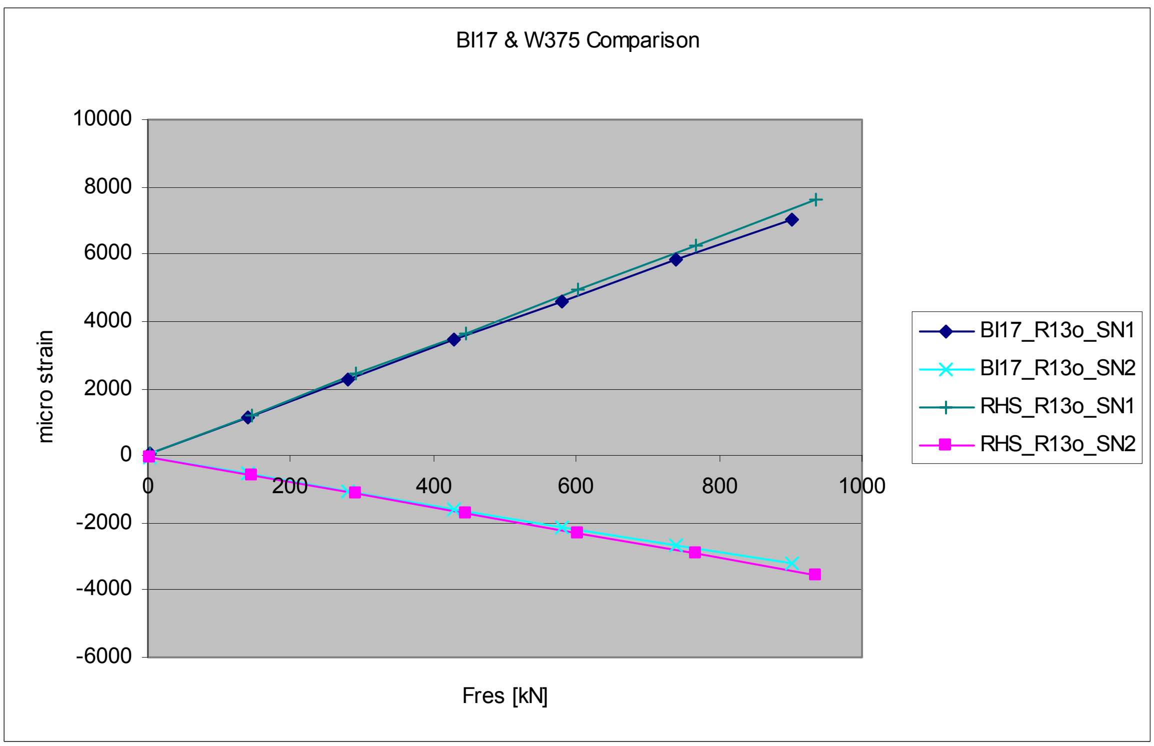

BI17_ = RHS ANSYS 3D model with scaled BI17 design gust load case
RHS_ = RHS ASNYS 3D model with W375 load vector scaled on the NASTRAN Fres

9. Summary

A local fine mesh 3D FEA model has been created for the rear main lug area by ANSYS and translated to NASTRAN. This model has been inserted as the RHS & LHS (mirror image) into of the 2D global Vertical Stabilizer model.
The comparison with the pure 2D model revealed that the change of the attachment load distribution between front, center and rear lug is negligible, but the bending moment is reduced significantly. The displacements at the interface of the embedded RHS 3D rear lug model and the displacement of the fuselage clevis was used to perform a nonlinear contact analysis with ANSYS. Due to the contact behavior the lug bending moment was reduced further.
As expected, the analysis with displacement boundary conditions results in a further reduction of the bending moment and 9% percent lower attachment force resultant.
The chosen approach to scale the results to the linear NASTRAN resultant force W375 gives a bending moment Mx which is 8% lower than the value of the linear NASTRAN analysis with 180° bonded pin.
In addition the design gust load case BI17 was analyzed up to the Fres level of the full scale test rupture value. It is shown that the strain level around the right hand side rear pin hole is nearly identical to the strain level of the W375 load case.